UNITED STATES DEARTMENT OF THE INTERIOR

GEOLOGICAL SURVEY

Formation and resulfidization of a South Texas Roll-type uranium deposit

By

Martin B. Goldhaber,

Richard L. Reynolds,

and Robert O. Rye

Open-File Report 79-1651

1979

Contents

Table

Illustrations

Illustrations--continued

Formation and resulfidization of a South Texas roll-type uranium deposit

by Martin Goldhaber, Richard Reynolds, and R. O. Rye

Abstract

Core samples from a roll type uranium deposit in Live Oak County, south Texas have been studied and results are reported for Se, Mo, FeS_2 and organic-carbon distribution, sulfide mineral petrology, and sulfur isotopic composition of iron-disulfide phases. In addition, sulfur isotopic compositions of dissolved sulfate and sulfide from the modern ground water within the ore bearing sand have been studied. The suite of elements in the ore sand and their geometric relationships throughout the deposit are those expected for typical roll-type deposits with well-developed oxidation-reduction interfaces. However, iron-disulfide minerals are abundant in the altered tongue, demonstrating that this interval has been sulfidized after mineralization (resulfidized or rereduced). Iron disulfide minerals in the rereduced interval differ mineralogically and isotopically from those throughout the remainder of the deposit. The resulfidized sand contains dominantly pyrite that is enriched in ^{34}S, whereas the sand beyond the altered tongue contains abundant marcasite that is enriched in the light isotope, ^{32}S. Textural relationships between pyrite and marcasite help to establish relative timing of iron disulfide formation. In reduced rock outside the altered tongue, three distinct generations of iron disulfide are present. The oldest of these generations consists largely of pyrite with lesser amounts of marcasite. A major episode of marcasite formation contemporaneous with ore genesis postdates the oldest pyrite generation but predates a younger pyrite generation. Resulfidization probably led to the final pyrite stage recognized beyond the altered tongue. Stable isotope data establish that the source of sulfur for the resulfidization was fault-leaked H_2S probably derived from the Edwards Limestone of Cretaceous age which underlies the deposit.

The deposit formed in at least two stages: (1) a pre-ore process of host rock sulfidization which produced disseminated pyrite as the dominant iron disulfide phase; and (2) an ore-stage process which led to the development of the uranium roll with emplacement of the characteristic suite of minor and accessory elements and which produced abundant isotopically light marcasite. The host rock was modified by a post-ore stage of resulfidization which precipitated isotopically heavy pyrite. Sulfur isotopic compositions of sulfide and sulfate present in modern ground water within the host sand differ greatly from sulfur isotopic composition of iron disulfides formed during the resulfidization episode. Iron disulfide minerals formed from the sulfur species of modern ground water have not been unequivocally identified.

Introduction

Roll-type uranium deposits possess several features in common (Adler, 1974, Rackley, 1972). The ore host is a relatively permeable sandstone aquifer bounded above and below by less permeable, generally shaley strata. The ore occurs in curved layers that assume discordant C-shapes in cross section. The concave edge is normally sharp whereas the convex side is not and contains decreasing uranium content away from the concave margin. Host beds on the concave side of the ore roll typically have been epigenetically altered by flowing oxygenated ground water which also carried soluble hexavalent uranium. These altered rocks, typically tan to red in color, contain more ferric iron and less pyrite, organic carbon and mineral carbon than the same beds, typically gray in color, farther down the paleohydrologic gradient (downdip). The concave edge of the roll, therefore, represents an interface between oxidized and reduced geochemical environments. During active ore deposition, this interface acted as a geochemical redox barrier at and beyond which soluble hexavalent uranium was reduced to the tetravalent state and precipitated. Many of the associated and minor elements of these deposits such as S, Se and Mo are those whose chemistry, like U, is associated with higher solubility in an oxidized rather than a more reduced compound (Harshman, 1974). The uranium roll migrated down the paleodip as a result of oxidation and solubilization of ore constituents near the concave edge and reprecipitation in reduced rock. This migration led to the establishment of a progressively lengthening altered (oxidized) tongue of rock on the updip side of the roll and an enrichment of uranium ore grade in the roll as uranium bearing ground water flowed past the redox interface.

Reducing conditions on the downdip side of the redox boundary may result from the presence of organic matter (Rackley, 1972). In some south Texas deposits that lack organic matter, H_2S (and possibly hydrocarbon bearing fluids) derived from underlying oil and gas reservoirs and injected into the host beds during the ore-forming episode may be capable of directly precipitating uranium (Eargle and Weeks, 1961; Klohn and Pickens, 1970). Alternatively, the presence of iron disulfide (FeS_2) minerals engendered by fault-derived H_2S may provide an environment favorable for uranium concentration. In this situation, ore deposition may occur in the absence of sulfur-enriched gas and fluid with a deep seated source, as has been demonstrated for the Benavides deposit near Bruni in Webb County, Texas (Goldhaber and others, 1978).

Reduction-oxidation relationships developed during the ore-forming episode may be modified by later introduction of reduced sulfur bearing solutions into the host rock (Adler and Sharp, 1967; Dickinson and Duval, 1977; Galloway, 1977). Post-mineralization resulfidization of iron disulfide minerals oxidized during ore formation (rereduction) would presumably not lead to massive redistribution of ore constituents and accessory elements such as Mo because they are generally insoluble in their reduced forms. However, resulfidization processes may result in precipitation of iron disulfide minerals in the former oxidized tongue, and may, therefore, obscure mineralogic and color differences that had previously developed across the redox interface during mineralization.

No page 3

In this paper, we report on the geochemistry and sulfide mineralogy of a resulfidized deposit and formulate a genetic history of the deposit with emphasis on the source of reductants and timing of reduction episodes. In addition, we note geochemical and mineralogic characteristics of the deposit that may be useful in guiding exploration for similar resulfidized roll-type ore bodies.

Description of the deposit and sample suite

The uranium deposits of south Texas are found in the principal sand units of the Tertiary strata of the Gulf Coastal plain. The regional strike of the beds generally parallels the shoreline of the Gulf of Mexico (fig. 1), and the beds dip gently and thicken southeasterly toward the Gulf of Mexico.

The Lamprecht ore body is in Live Oak County and occurs in the basal sands of the Miocene Oakville Sandstone. The host sand is bounded below by mudstone of the Catahoula Tuff (fig. 2). The ore sand is overlain by a sequence of intercalated beds of sand and clay (fig. 2), which in the area of the mine, are laterally continuous. They are interpreted as having been deposited primarily in a channel margin, overbank environment. The Oakville crops out within a distance of about 2.5 km northwest of the Lamprecht mine site.

A normal fault (downthrown coastward) occurs downdip from and is subparallel to a portion of the roll front (fig. 3). Several other deposits bear a conspicuous spatial relationship to this fault (fig. 3). Additional faults also may have controlled ore localization in this area, as for example at the Kopplin mine. (fig. 3).

Samples were obtained from 9 cores along a fence drilled nearly perpendicular to the trend of the roll front (fig. 4). The distance between core 1 (the farthest updip) and core 10 (the farthest downdip) is approximately 1350 m. The ore roll containing the highest uranium content is between cores 5 and 6. Samples representing depth intervals of between 0.15 m and 0.3 m had been separated and aliquots of these treated with bromoform to obtain the heavy-mineral fractions prior to our study.

Samples of ground water from the mine area were obtained from monitor wells cased down to the ore sand interval. These wells are sufficiently remote from mining activity as to be undisturbed by it. Water was pumped from these wells until the conductivity stabilized, and then approximately 500 ml of water was transferred into polyethylene bottles previously prepared with a known amount of cadmium acetate. Dissolved sulfide present in the water is preserved as cadmium sulfide by this technique (Goldhaber, 1974). Additional data on ground-water composition at the Lamprecht and the adjoining Zamzow mine was obtained from public documents filed with the Texas Water Quality Board in Austin, Texas.

Laboratory Procedures

Subsamples of the heavy mineral suite were mounted in epoxy and polished for viewing under oil by reflected-light microscopy. More than 250 polished sections were examined during the course of the study. Marcasite and pyrite were identified by their distinctive optical properties, and their relative proportions were estimated visually by two independent observers. Additional

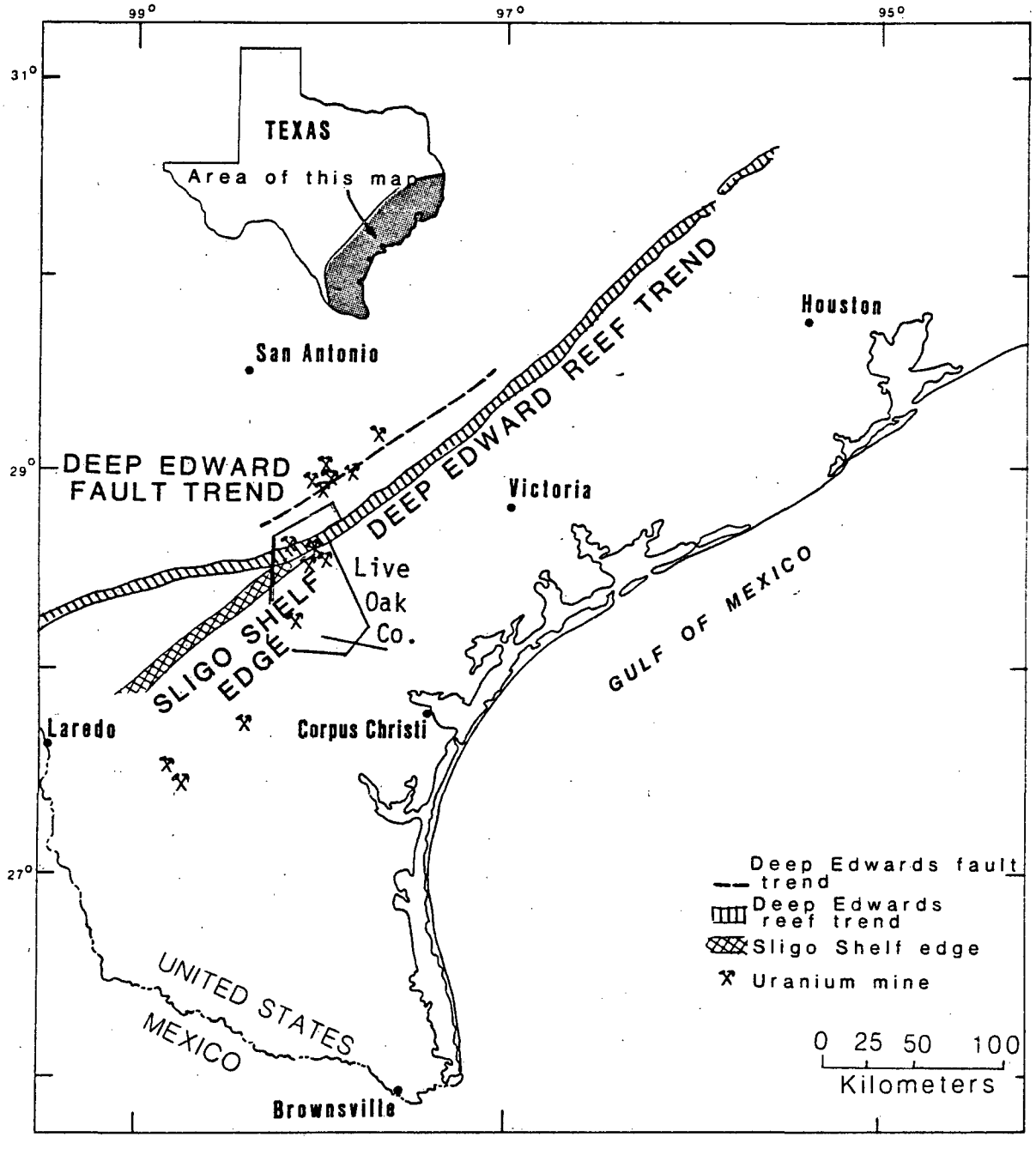

Figure 1.--Geologic map of the south Texas coastal plain showing the outcrop belt of uranium-bearing formations, uranium mines, and prospects. Modified from Dickinson (1976). Also shown is the surface projection of Cretaceous Edwards carbonate reef trend and deep Edwards fault trend (data from Rinehart, 1962) and the Cretaceous Sligo shelf edge (data from Bebout, 1977).

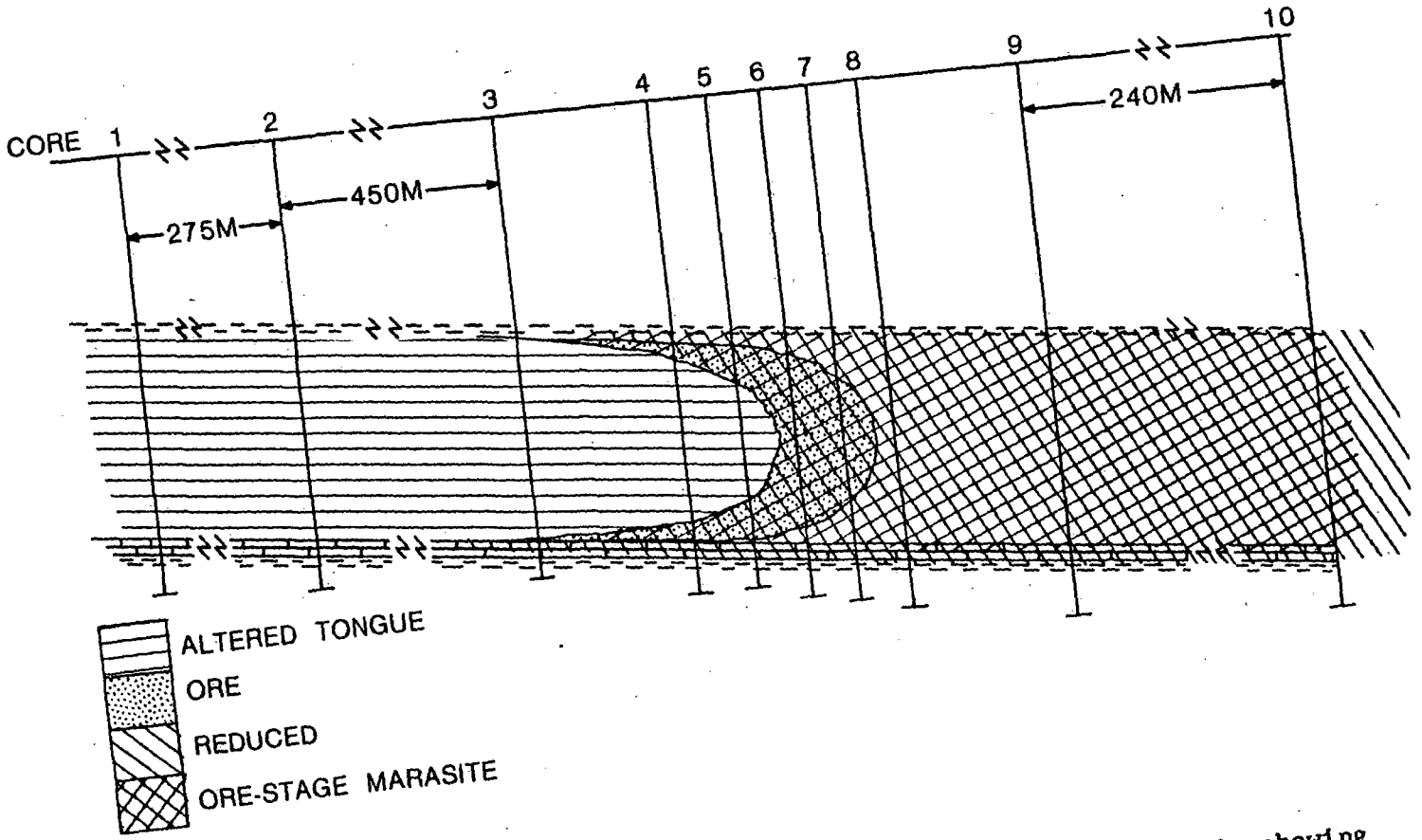

Figure 2.--Lithologic cross section through the Lamprecht deposit showing location of roll front and exploration drill holes in the Oakville Sandstone. Hole 11 was not cored. Source of information is Wyoming Mineral Corporation (unpub. data).

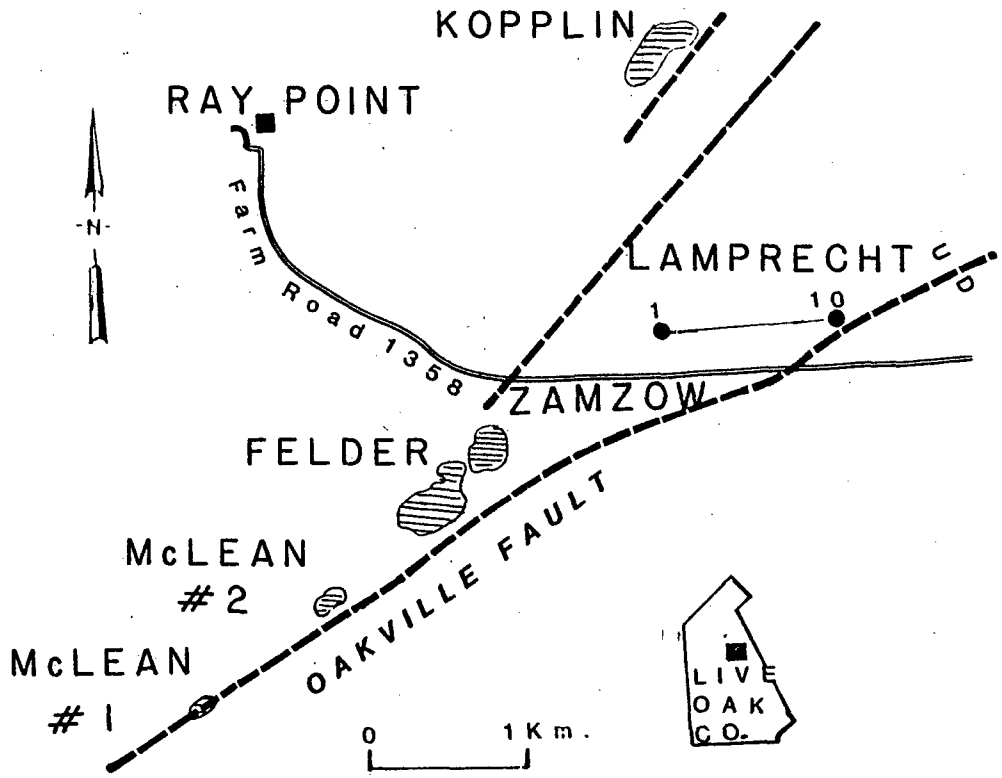

Figure 3.--Plan view of the Ray Point area, Live Oak County, Texas (shaded portion of location map), showing deposits along the Oakville and adjacent faults. The approximate outlines of open pit mines (shaded) are shown except in the Zamzow deposit and the Lamprecht deposit which are being solution mined. The relationship of the core fence (cores 1 and 10 shown here; fig. 2) to the Oakville Fault is shown for reference.

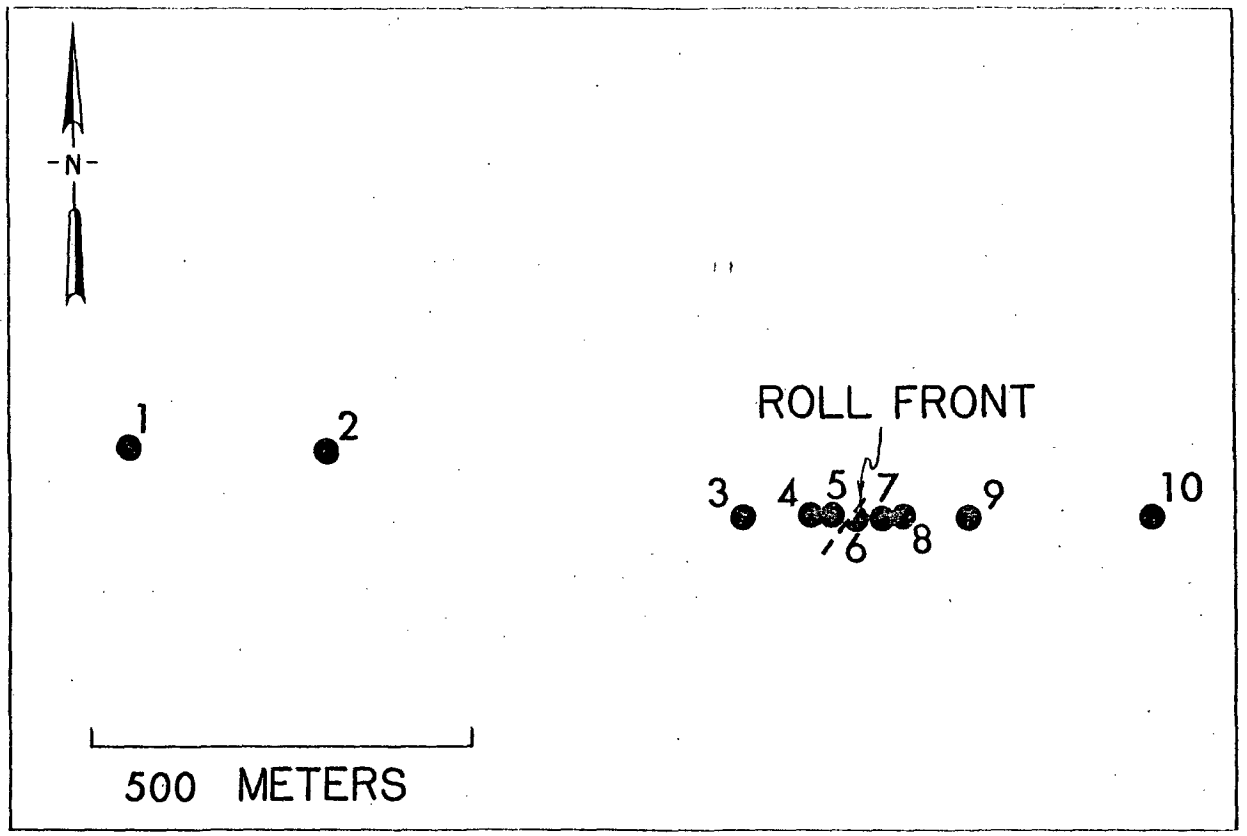

Figure 4.--Plan view of core fence drilled across Lamprecht ore body (1-10), showing the spacing of core holes and location of roll front.

subsamples of the heavy mineral suite were prepared for stable-isotope analyses. These were treated with hydrochloric acid to remove carbonates and oxides, and by hydrofluoric acid to remove silicates. We have previously demonstrated that these reagents do not appreciably attack pyrite and marcasite under the conditions employed (Goldhaber and others, 1978). The resulting FeS_2-rich concentrate was combusted in oxygen to yield SO_2 for isotopic analysis which was performed on a Nuclide^R 6"-radius 60°-sector mass spectrometer. Results are reported in delta notation which is the permil deviation of the isotope ratio $^{34}S/^{32}S$ from the ratio of a standard (Cañon Diablo troilite). Precision of this technique is ±0.2 permil.

The chemical data for Mo and Se were supplied by Wyoming Mineral Corporation and were determined by wet-chemical techniques. Organic carbon was determined on a selected suite of samples using the LECO^R induction-furnace technique after removal of carbonate carbon in dilute hydrochloric acid.

Ground-water samples were analyzed for their content of dissolved sulfide and sulfate. Sulfide was determined by precipitation with cadmium, followed by filtering the cadmium sulfide precipitate and placing it in a reaction vessel. Hydrochloric acid (6N) was added and the resulting hydrogen sulfide gas stripped from the reaction vessel and precipitated as silver sulfide in a silver nitrate trap and subsequently weighed. Sulfate was determined gravimetrically as barium sulfate in the sulfide-free supernatent solution. The barium sulfate and silver sulfide were converted to SO_2 gas for isotopic analysis of sulfate and sulfide sulfur, respectively.

Results

Chemistry

In cross section, the uranium-enriched zone occurs in a C-shaped roll (fig. 2). The highest concentrations of uranium occur in the ore roll in core 6 at depths of 70 to 79 m and in core 7 (fig. 5) at 70.7 to 80.2 m. Uranium enrichment also occurs in upper and lower limbs updip from the nose of the roll in cores 4 (fig. 6) and 5. Host rock between the upper and lower limbs (71-77 m in core 4), as well as host rock occupying a comparable position in core 3 and 5, represents a zone normally referred to as the altered (oxidized) tongue or alternatively, the barren interior.

Molybdenum and selenium are diagnostic elements whose geochemistry and distribution is indicative of the nature of the ore forming process (Harshman 1974). For illustrative purposes, we have plotted selenium (figs. 7, 8) and molybdenum (figs. 9, 10) data from the host sand interval of cores 4 and 7. Selenium enrichment in core 4 is localized for the most part in the altered tongue, but some enrichment occurs additionally in the upper and lower limb ore. Molybdenum, on the other hand, is enriched both above and below the altered tongue in the ore limbs and is largely coextensive with uranium. In core 7, selenium content is extremely low (mostly less than 2 ppm), molybdenum is abundant (as much as 240 ppm). The geometric relationships of selenium and molybdenum together with the distribution of uranium in a roll morphology, are typical of those observed in roll-type deposits and are indicative of an ore-forming process in which oxidizing (oxygenated) solutions carrying these elements progressively encroached into a reducing enyironment (Harshman, 1974).

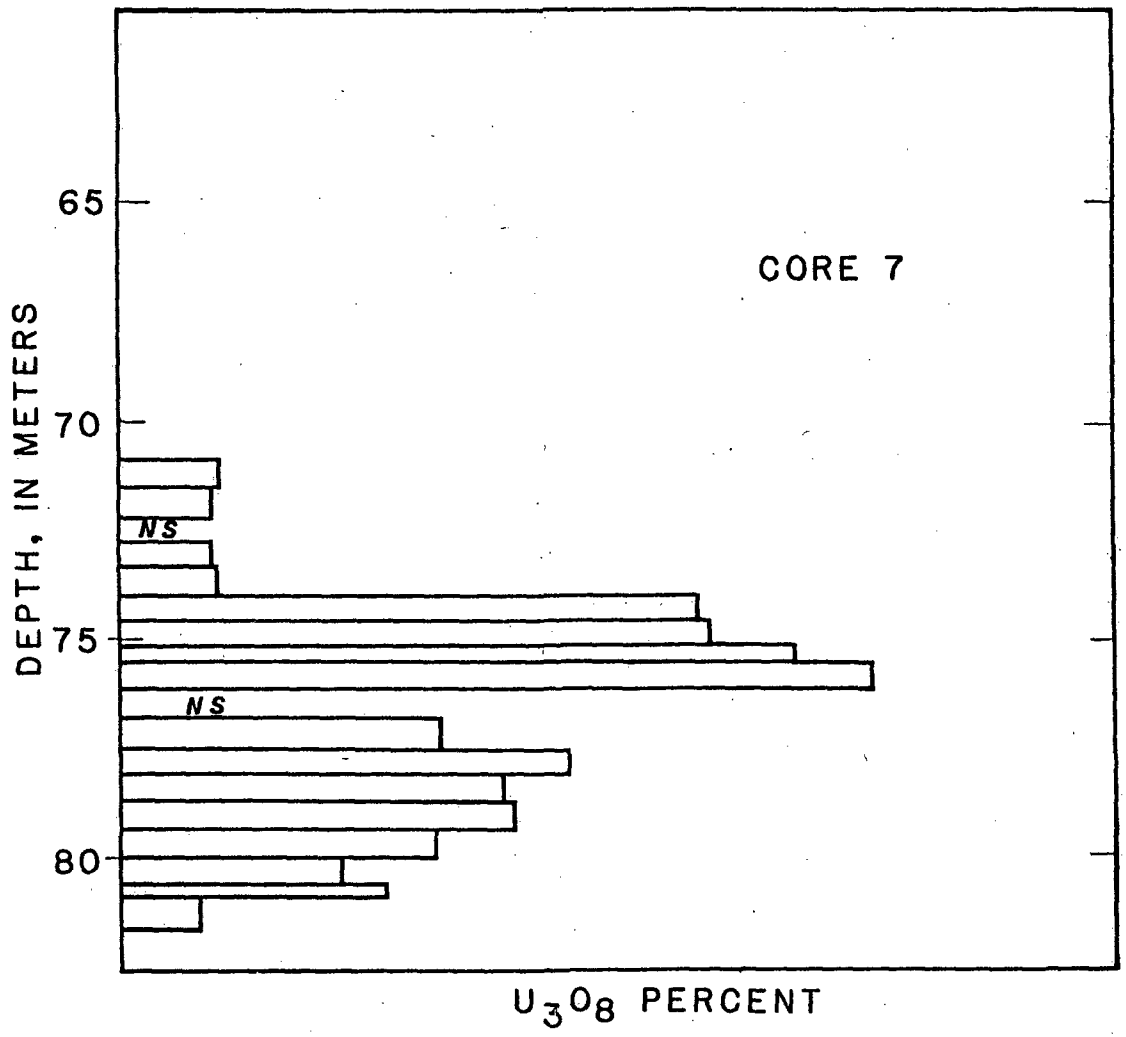

Figure 5.--Uranium concentration shown as percent U_3O_8 on a log scale against depth through the host sand of core 7. Actual uranium data withheld at company request. The uranium enrichment throughout much of the ore-sand interval is typical for roll-type uranium deposits. Here and in following plots, NS stands for no sample.

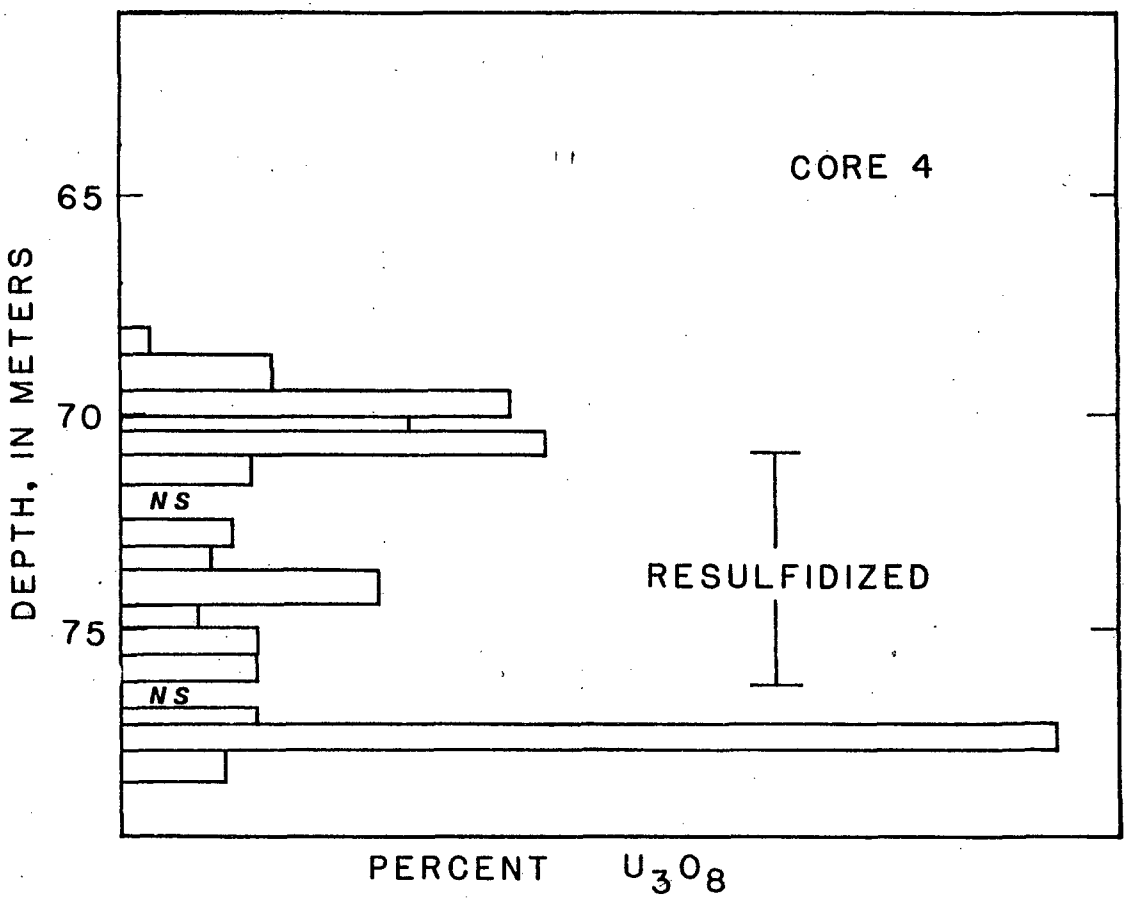

Figure 6.--Uranium concentration shown as percent U_3O_8 on a log scale against depth through the ore-sand horizon of core 4. Actual uranium data withheld at company request. The uranium enrichment in upper and lower "limbs" is typical for roll-type deposits.

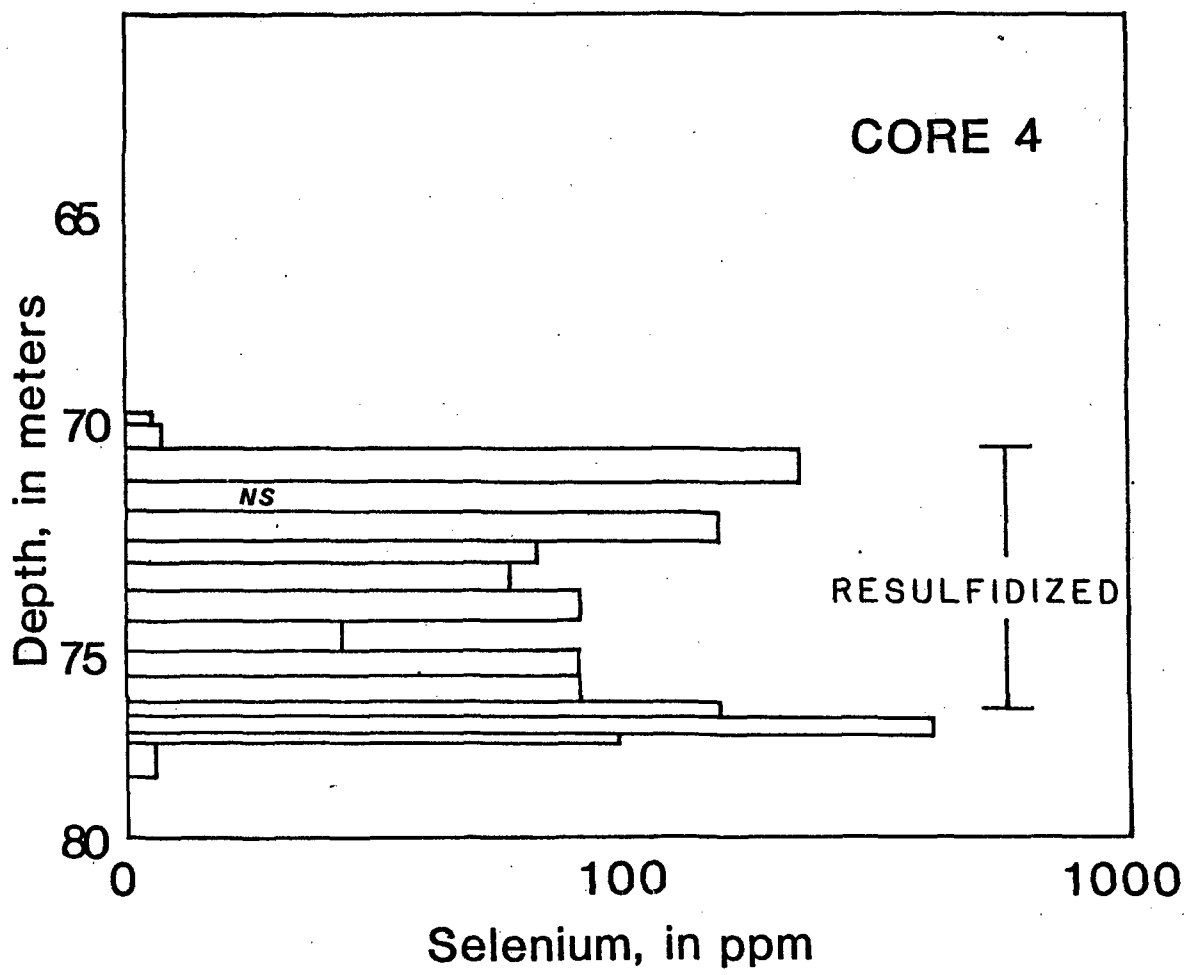

Figure 7.--Selenium concentration shown on log scale against depth for core 4 showing selenium enrichment within the altered tongue and into reduced rock as is typical for roll-type uranium deposits.

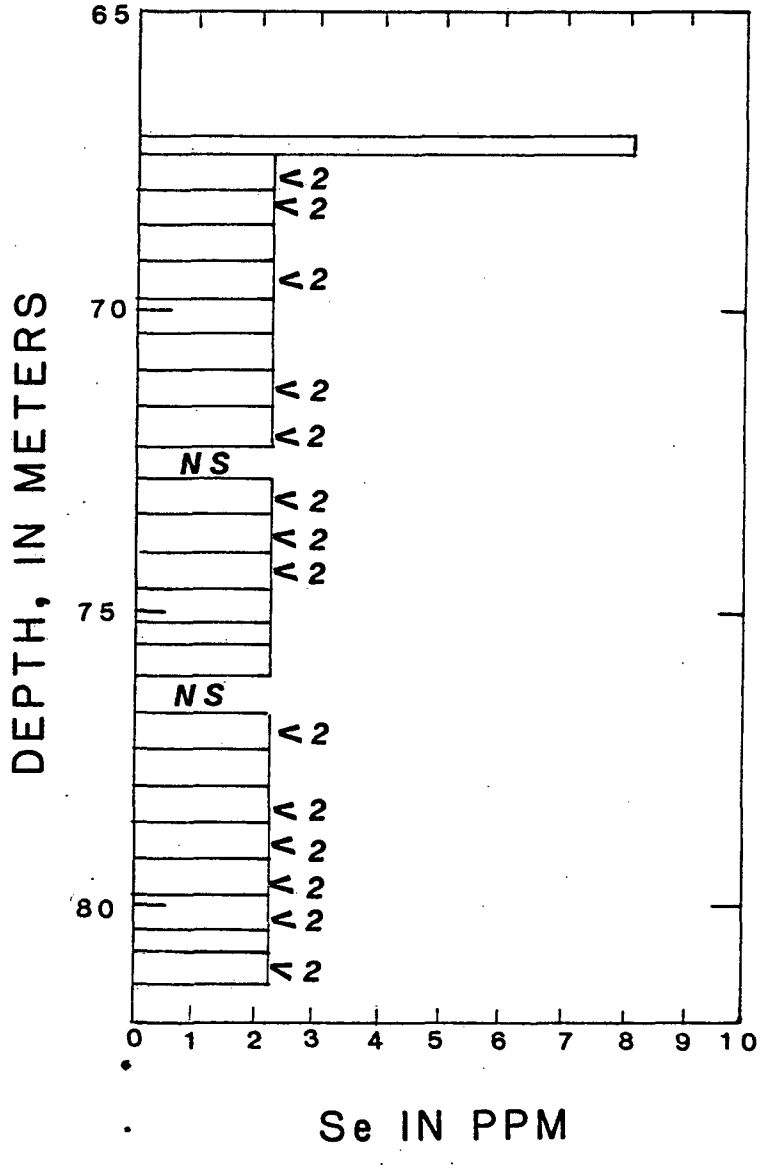

Figure 8.--Selenium concentration shown against depth for core 7. Lack of selenium enrichment in the ore roll downdip from the resulfidized interval can be seen.

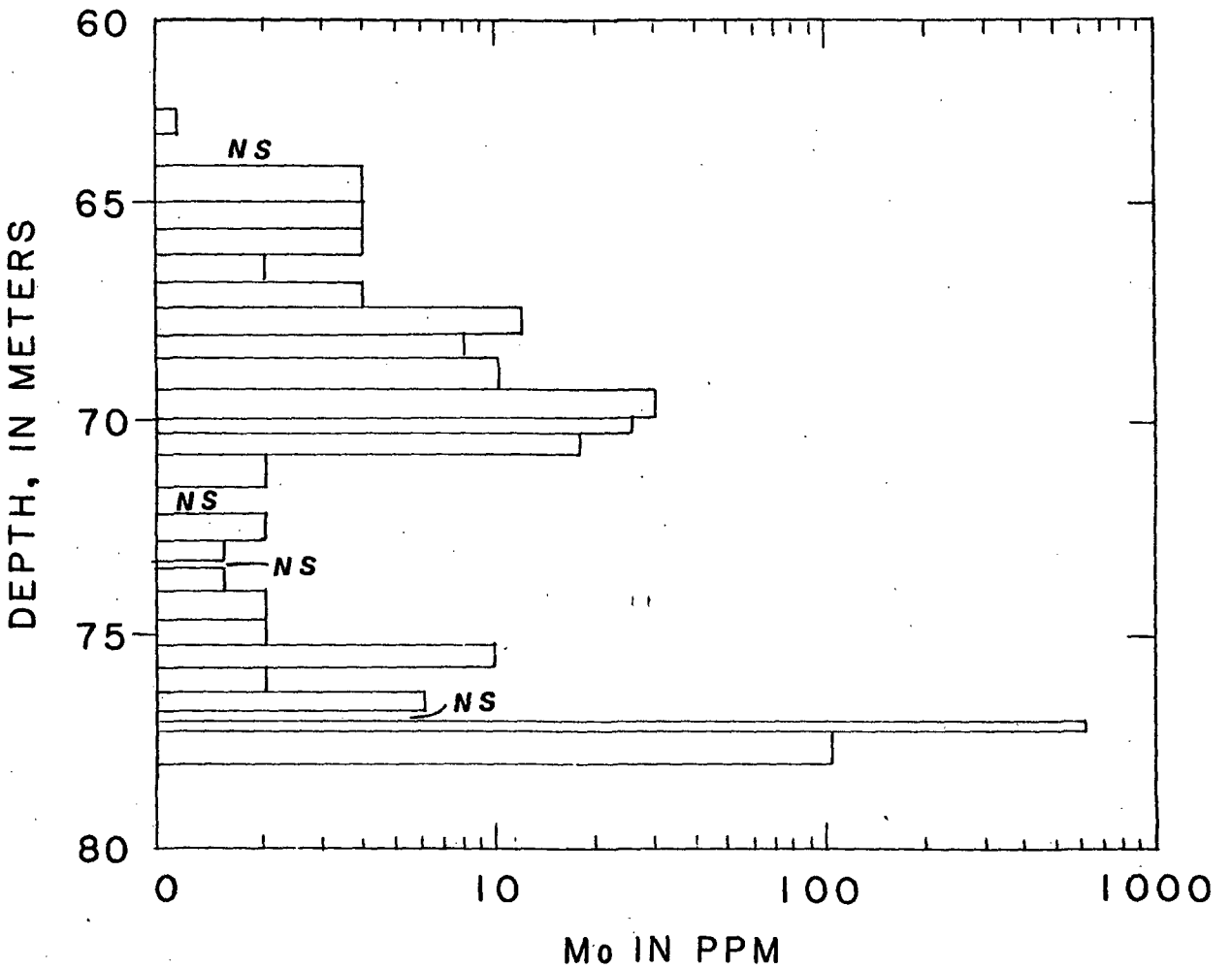

Figure 9.--Plot of molybdenum concentration shown on log scale against depth for core 4 illustrating molybdenum enrichment in upper and lower limbs.

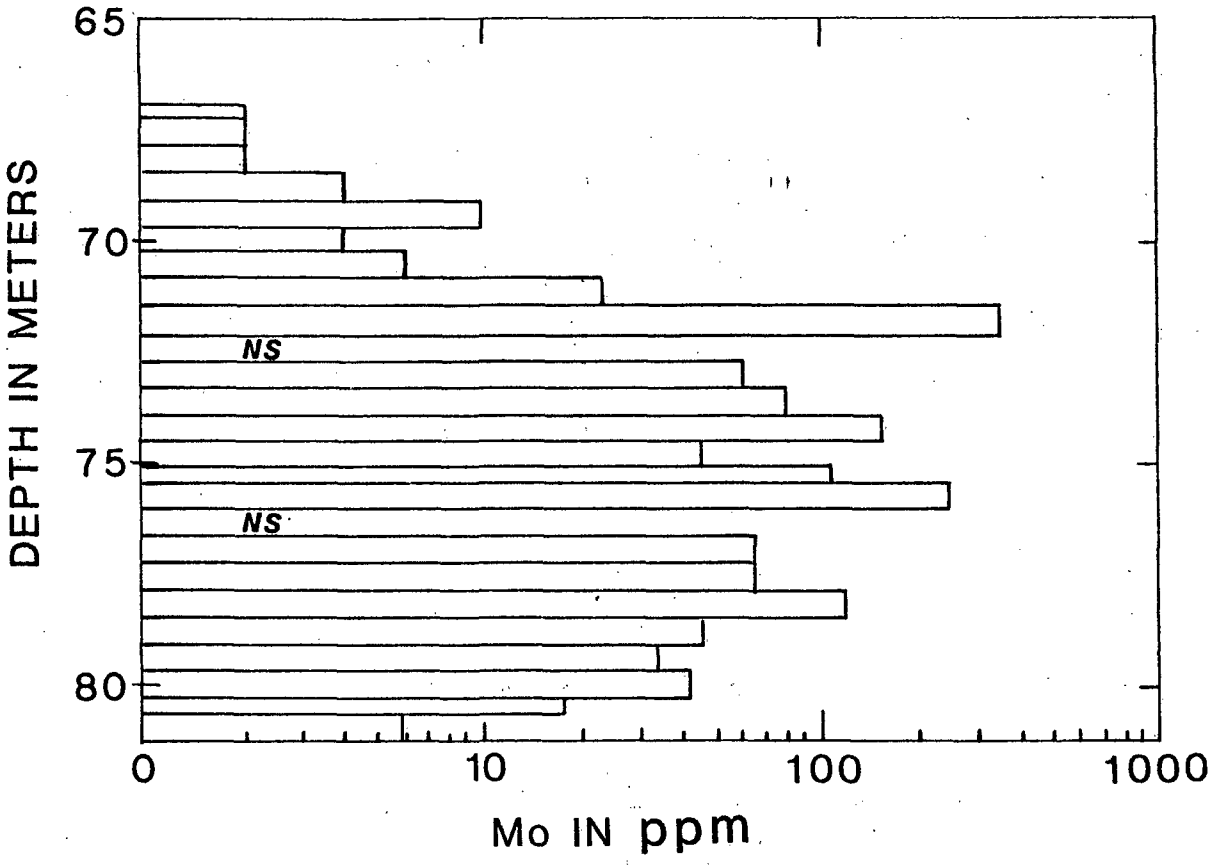

Figure 10.--Plot of molybdenum concentration on a log scale against depth, core 7, illustrating molybdenum enrichment through the host sand in the portion of the ore roll downdip from the resulfidized interval.

Results of organic carbon analyses are contained in table 1. Of the 26 samples analyzed, only three contained organic carbon at detectable levels although only small amounts were present. Of these three, two were mudstones: one above the ore sand in the Oakville and one below it in the uppermost Catahoula. Two additional mudstone samples from the Catahoula did not contain detectable organic carbon, nor did two additional Oakville mudstone samples. The virtual absence of organic matter within the Oakville ore sand and very low values in adjacent mudstones precludes major microbiological activity involving sulfate reduction within these zones (Goldhaber and others, 1978).

Ground-water geochemistry

The distribution of total dissolved solids (TDS) in ground water of the ore-sand interval of the Lamprecht and adjoining Zamzow deposits is plotted in figure 11. These data show a complex pattern of recharge-discharge or mixing of differing water types in the area of the mines. There is a general tendency for TDS on the Zamzow property to show a symmetrical distribution on either side of the Oakville fault with TDS increasing away from each side of the fault. On the south side of the fault, this increase is followed by a decrease at greater distances. In general, the Lamprecht data from the north side of the fault resembles those from Zamzow. TDS values from further northwest of the mine towards the outcrop (Wyoming Mineral Corp., unpub. environmental impact statement) tend to be lower than those from near the mine, implying that a decrease in TDS continues as the recharge (outcrop) area is approached.

Superimposed upon these general trends are anomalous zones near the fault which may represent tongues of water of higher TDS content derived from either deeper (?) formations or, as discussed below, possibly from surface recharge processes. These tongues are documented south of the Oakville fault on the Zamzow property and north of the fault on the Lamprecht property. In addition, at Lamprecht, there is evidence for a zone of water of lower TDS content related to the fault.

Sulfate concentration in ground water is plotted in figure 12. In general, sulfate decreases with increasing distance from the fault. Exceptions to this trend are samples collected 83 and 112 m north of the fault. One of these samples is associated with the tongue of water of anomalously high TDS content which may be issuing from the fault. The $\delta^{34}S$ values of ground-water sulfate (fig. 13) show a tendency to become systematically heavier with distance from the fault as sulfate concentration decreases. The concentration and isotopic trends for sulfate both display the behavior expected for bacterial sulfate reduction. This process involves the preferential removal of isotopically light sulfur from the sulfate reservoir, forms sulfide, and leaves the residual sulfate reservoir enriched in ^{34}S (Goldhaber and Kaplan, 1974). Dissolved sulfide concentration (fig. 14) is relatively low in the vicinity of the fault, increases updip from the fault and then decreases again farther in the updip direction. The isotopic ratio of the dissolved sulfide tends to increase in samples at greater distances from the fault plane than in those close to it. (fig. 15). This behavior is also consistent with sulfide forming bacterially from a reservoir of sulfate which is itself becoming depleted in isotopically light sulfur.

Table 1.--Organic carbon content of samples from the Lamprecht deposit, south Texas

[Analyst, Van Shawe]

Core	Organic carbon as C in percent	Lithology
1	0.02	Shale; uppermost Catahoula Tuff.
2	.01	Carbonate rich sand.
2	.01	Shale above ore sand.
2	<.01	Do.
3	<.01	Ore sand
3	<.01	Do.
3	<.01	Do.
3	<.01	Shale; uppermost Catahoula Tuff.
4	<.01	Shale; Oakville Sandstone.
4	<.01	Ore sand.
4	<.01	Do.
4	<.01	Do.
4	<.01	Do.
4	<.01	Do.
4	<.01	Do.
4	<.01	Shale; uppermost Catahoula Tuff.
5	<.01	Ore sand.
5	<.01	Do.
5	<.01	Do.
5	<.01	Do.
9	<.01	Do.
9	<.01	Do.
9	<.01	Do.
10	<.01	Do.
10	<.01	Do.
10	<.01	Do.

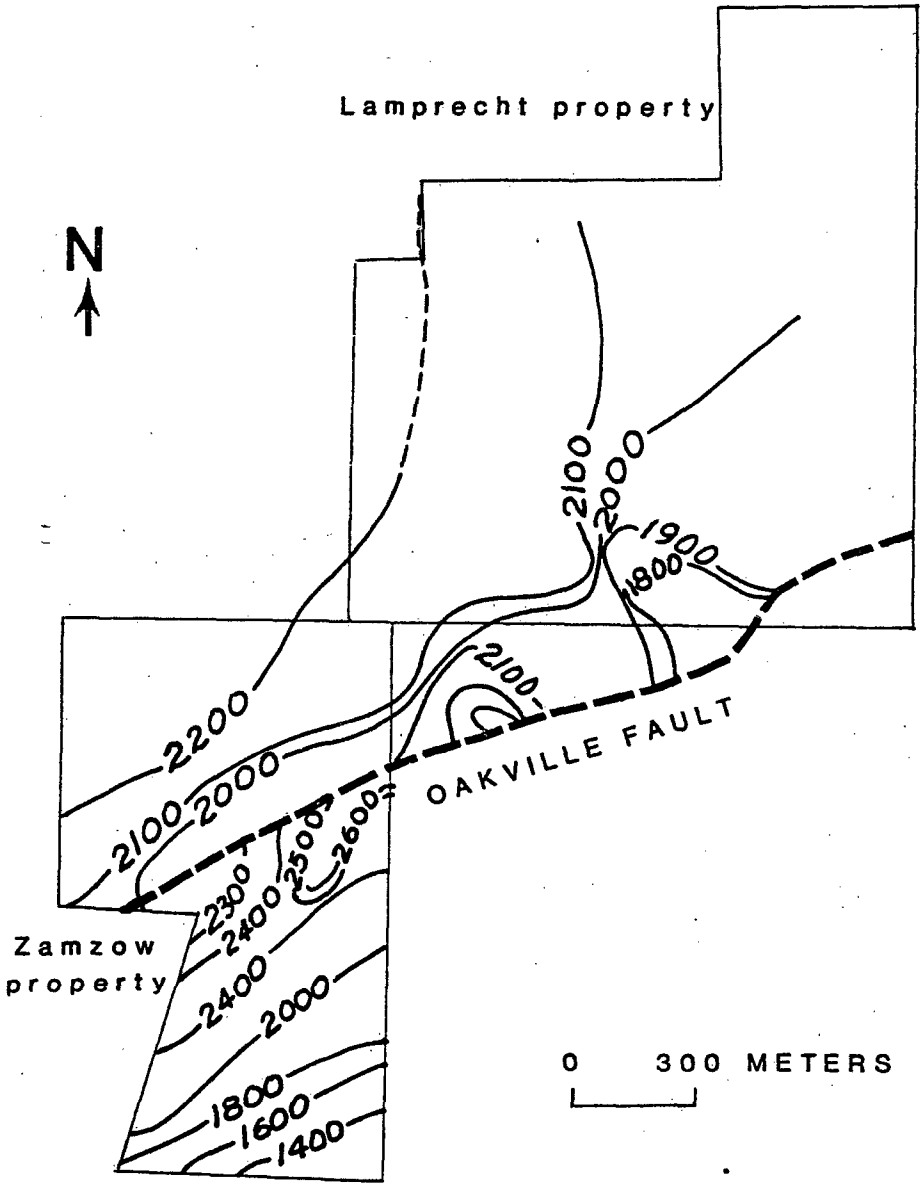

Figure 11.--Plan view of the Lamprecht and adjoining Zamzow properties showing contours (solid lines) of total dissolved solids (milligrams per liter) in the host sand. Data from 79 monitor wells. Note the relationship of tongues of both saline and fresher waters to the Oakville Fault (heavy dashed line).

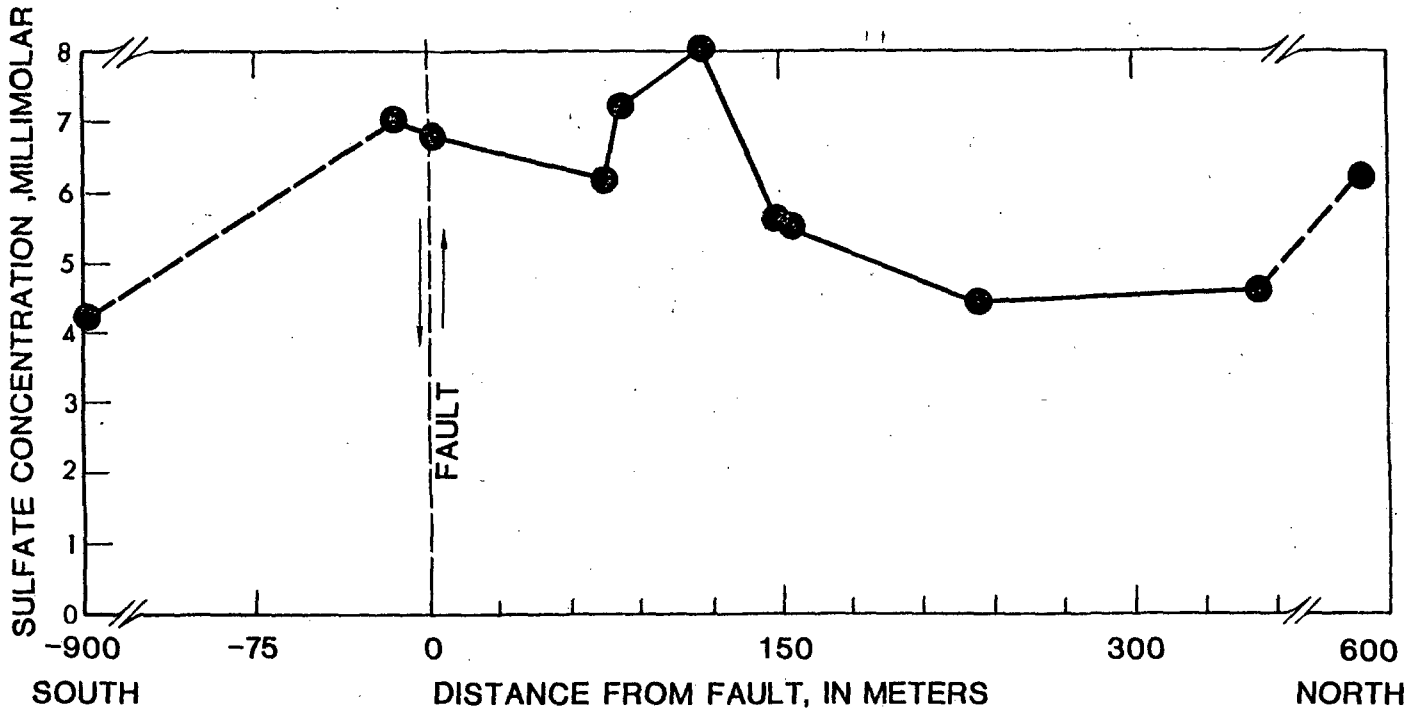

Figure 12.--Sulfate concentration in millimoles per liter plotted against distance (in meters) north of Oakville Fault (positive numbers) and south of Oakville Fault (negative numbers) for ground-water samples recovered from the host-sand interval.

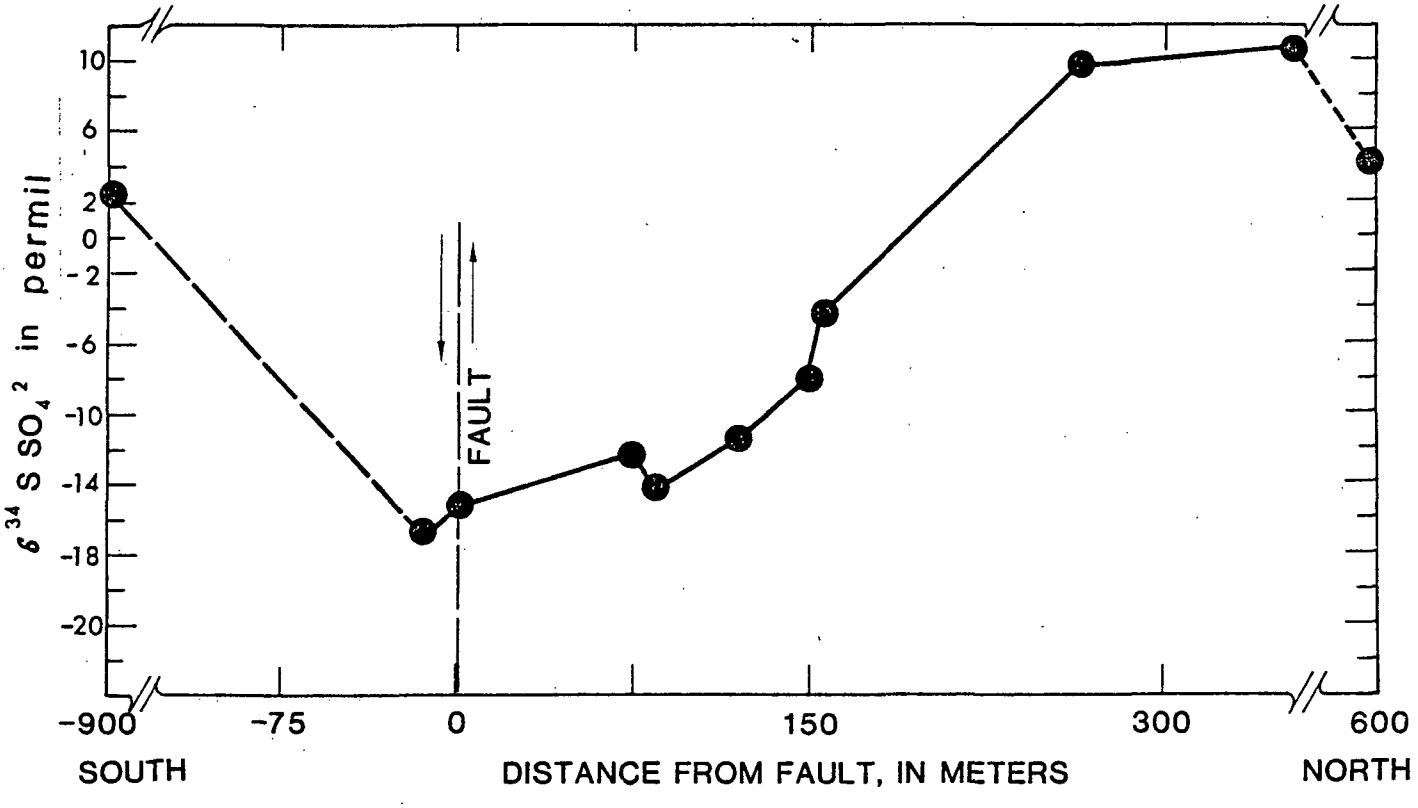

Figure 13.--Sulfur isotope ratio $\delta^{34}S$ of sulfate in ground-water samples shown in figure 12, illustrating increase in isotopic ratio away from the fault. U, upthrown side and D, downthrown side.

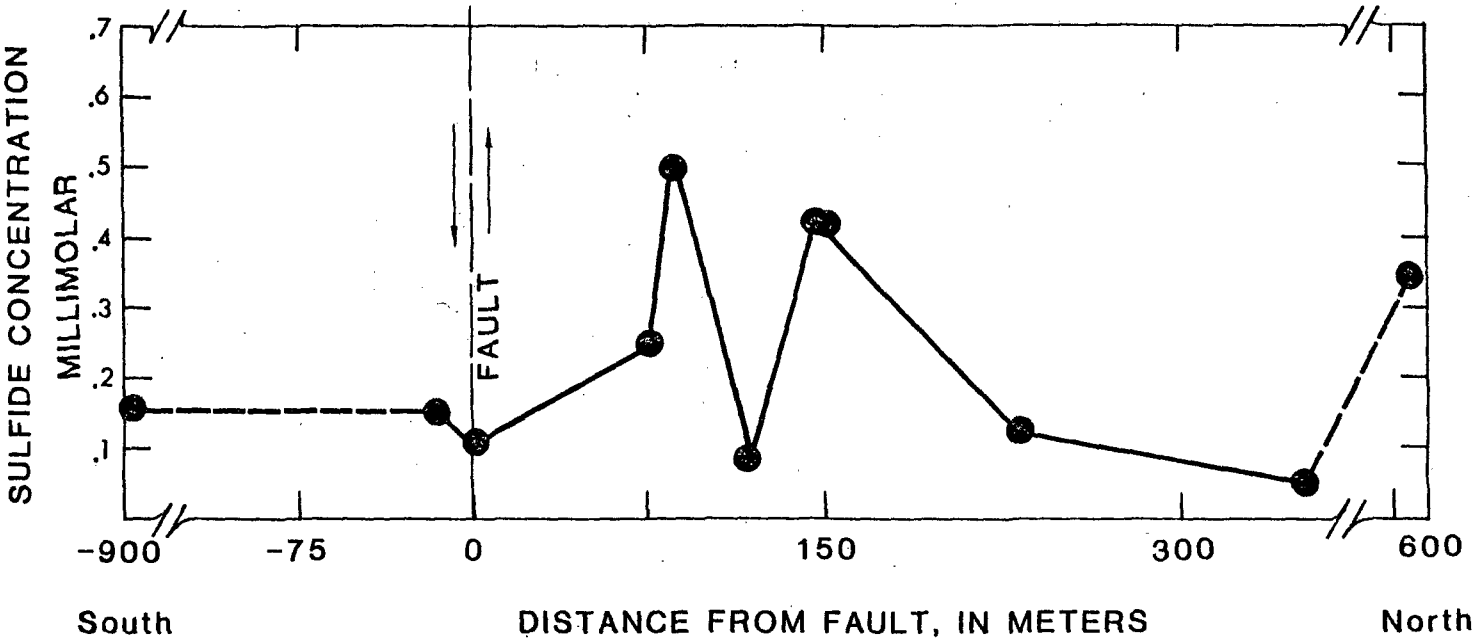

Figure 14.--Concentration of dissolved sulfide ($H_2S + HS^-$) in ground-water samples recovered from the host sand interval.

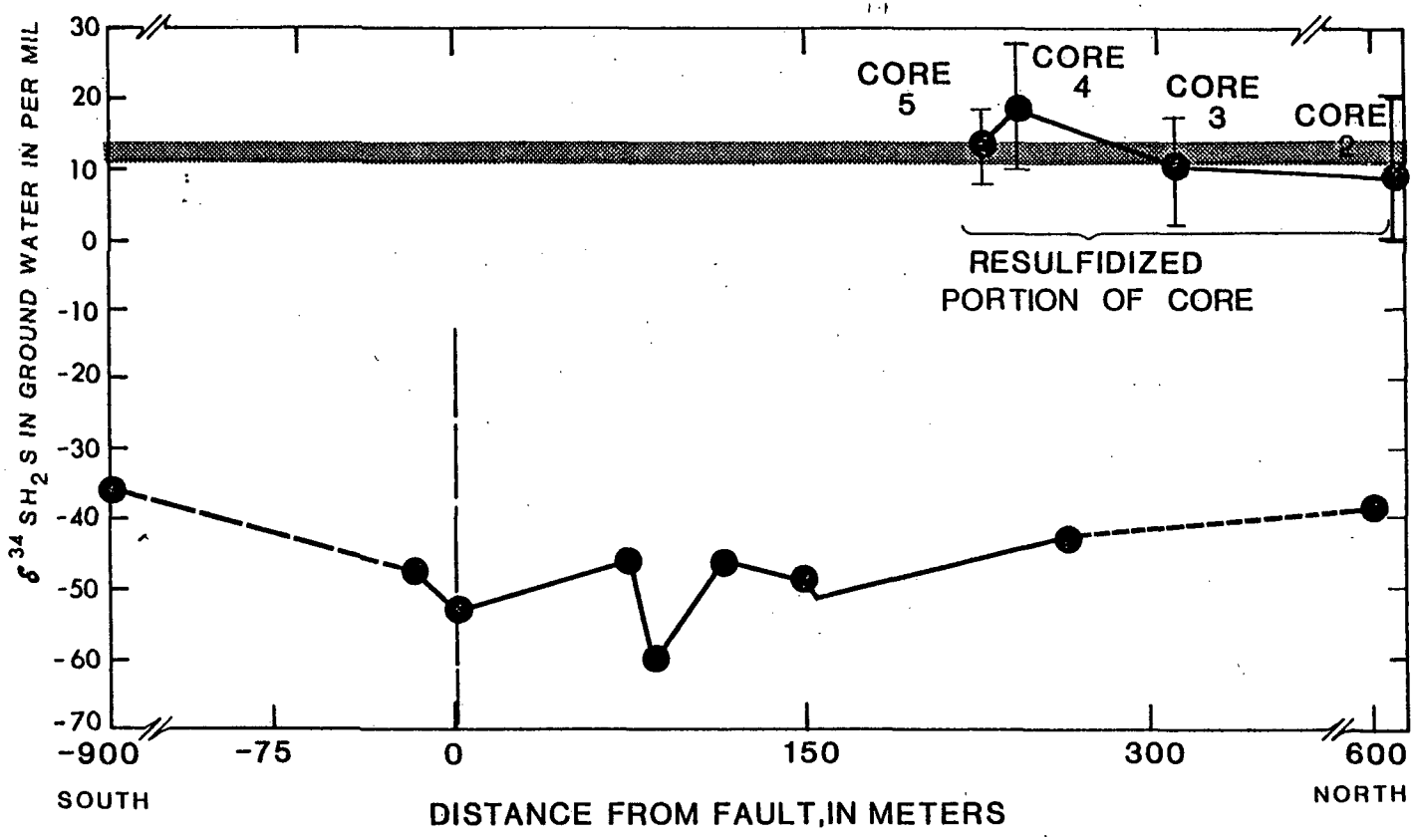

Figure 15.--Sulfur isotopic ratio, $\delta^{34}S$, of the dissolved sulfide in groundwater samples plotted in figure 14. Also shown for comparison are $\delta^{34}S$ values of iron-disulfide minerals in samples from the resulfidized interval. Core numbers of these solid phase samples are accompanied by the range of $\delta^{34}S$ values within the resulfidized zone (as a vertical bar).

Although the ground-water data are consistent with bacterial reduction, this hypothesis is at odds with the virtual lack of organic carbon in the host rock (table 1). Organic matter is required by sulfate reducing bacteria as noted above. Therefore, either organic matter is dissolved in the ground water recharging the area of the deposit, or some other process besides bacterial sulfate reduction is producing the dissolved sulfide. This alternative process might involve disproportionation reactions of metastable sulfur species arising from pyrite oxidation (Granger and Warren, 1969), and would produce trends in sulfate-sulfide concentration and isotopic ratios qualitatively similar to the bacterial pathway. Although we cannot presently distinguish between the two mechanisms of ground-water sulfide generation, some support for the inorganic pathway comes from data that pyrite oxidation is occurring in the vicinity of the fault.

Of particular interest in this regard is the observation that the ground-water sulfate in the vicinity of the fault is isotopically light (fig. 13). This is highly atypical for ground water sulfates (Rightmire and others, 1974), which normally have large positive $\delta^{34}S$ values. The light sulfate most probably reflects secondary oxidation of isotopically light iron disulfide minerals. The oxidation requires atmospheric oxygen and thus is likely to represent a surficial weathering process. In the nearby Felder mine (fig. 3), Klohn and Pickens (1970) have documented the partial secondary oxidation of an ore body by surficial weathering. This type of weathering may thus contribute to the ground water sulfate content. Percolation of oxygenated surface waters down the fault plane with migration of these waters out into the ore sand horizon is a mechanism which may account for the observed $\delta^{34}S$ values of ground water sulfate. This possibility is not contradicted by surface water data from nearby Sulfur Creek, which when sampled, had a high TDS content of 1700 mg/L, a $\delta^{34}S$ of -0.1 permil, and a sulfate concentration of 5.8 (mM). Assuming that this surface water is augmented in its sulfate concentration to 8.0 mM by oxidation of iron disulfide with a $\delta^{34}S$ value of -45 permil, the resulting sulfate in solution would have a $\delta^{34}S$ of -12.5 permil, and a TDS content of at least 1920 mg/L. The TDS would in fact be much greater than 1920 mg/L because acid released during oxidation of iron disulfide would dissolve large amounts of calcium carbonate and other phases. The predicted $\delta^{34}S$ of sulfate of-12.5 permil compares favorably with ground-water values near the fault which range between -12 to -17 permil.

The ground-water geochemistry discussed above, which involves a combination of sulfate addition via recharge down the Oakville fault and sulfide addition by bacterial reduction or inorganic mechanisms, is consistent with the overall trend in ground-water chemistry (fig. 16). Figure 16 is a plot of the ground-water sulfate content at Lamprecht plotted against the sulfate to chloride ratio of the same samples. This plot illustrates that sulfate, for the most part, varies independently from chloride as predicted by the proposed processes. This observation strengthens the case for a surficial source of isotopically light sulfate entering the fault from above rather than a deep seated "brine" source leaking up the fault. The latter would be associated with high chloride and isotopically heavy H_2S (see below). Ultimately, however, the high waters of high TDS content must in some fashion be related to deeper connate brines (W. Galloway, oral commun., 1977).

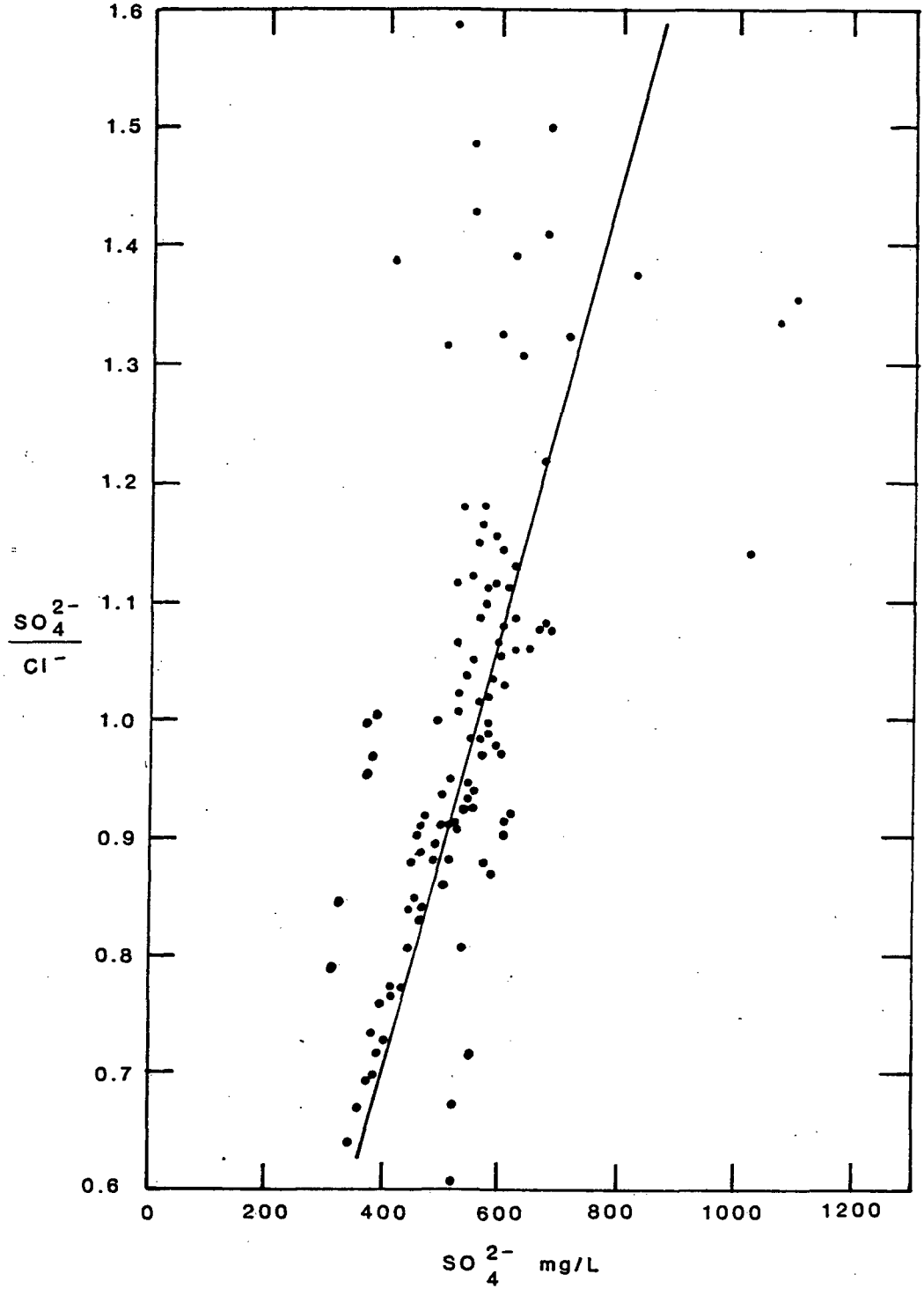

Figure 16.--Plot of the ratio of sulfate to chloride concentrations against sulfate concentration (expressed as milligrams per liter). The line drawn thru the data points reflects what would be expected for sulfate addition at constant chloride concentration.

Abundance and Distribution of Iron Disulfide Minerals

The iron disulfide minerals (pyrite and marcasite) are abundant throughout the deposit; individual samples may contain more than 2 weight percent FeS_2 (for example, fig. 17). Of particular interest is the presence of FeS_2 within the altered tongue. This is illustrated in figure 17, which shows the abundance of FeS_2 minerals in core 4. Iron disulfides in the altered tongue (71-77 m in core 4), although less abundant than in sands stratigraphically above this level, are present in significant quantities (0.3-1.4 percent FeS_2). The lower limb beneath the altered tongue is for the most part in mudstone, and is, therefore, not directly comparable to overlying sands. Iron disulfide mineral content is also systematically lower in the altered tongue than in overlying sand in cores 2, 3 and 5. In figure 18 the average (mean) iron disulfide contents within the rereduced altered tongue, ore zone and reduced barren rock are plotted as functions of core position.

The presence of FeS_2 minerals within the altered tongue is indicative of a post-mineralization episode of sulfidization (resulfidization), and the altered tongue will be referred to hereafter as the resulfidized interval. The high concentrations of iron disulfide minerals in sands that lack organic matter and, therefore, that lack bacterial sulfide suggest an extrinsic source of sulfide throughout most of the deposit.

Sulfide mineralogy

Systematic variations in the relative proportions of pyrite and marcasite have been observed within the host sand. Samples at or downdip from the nose of the roll (cores 6 to 10) contain dominantly marcasite. A typical distribution in one of these cores (core 7) is shown in figure 19.

Marcasite is greater than 50 percent of the total iron disulfide population throughout core 7 except in a mudstone layer (at depths of 64.5-66.5 m) which is relatively enriched in pyrite. The mudstone layer appears to be laterally continuous and where sampled in other cores is typically more pyritiferous than sands stratigraphically above and below.

Similarly, marcasite is the dominant iron disulfide mineral in rock above and below the rereduced interval-again with the exception of the more pyritiferous mudstone. Within the rereduced interval, however, pyrite is much more abundant than marcasite in cores 4 and 5 (figs. 20,21). A marked distinction between rereduced rock and rock in cores 6 to 10 is apparent (fig. 22).

Textures of iron-disulfide minerals

At least three and perhaps four temporally different generations of iron-disulfide minerals have been identified in the Lamprecht host sands. Distinct textural and spatial relationships among the three generations exist in cores 3, 4, and 5, each of which penetrates the resulfidized interval, the bounding ore limbs and reduced rock above and below ore. Above and below the resulfidized zone in these cores, individual grains are comprised commonly of iron disulfide representing each generation. These grains almost invariably consist of an inner nucleus of pyrite, an overgrowth of marcasite (as much as 20 m thick) surrounding the pyrite nucleus, and an outer rim of pyrite overgrown on the marcasite. The nucleus, representing the earliest identifiable sulfide generation, may consist of large (as much as 150 μm) subhedral

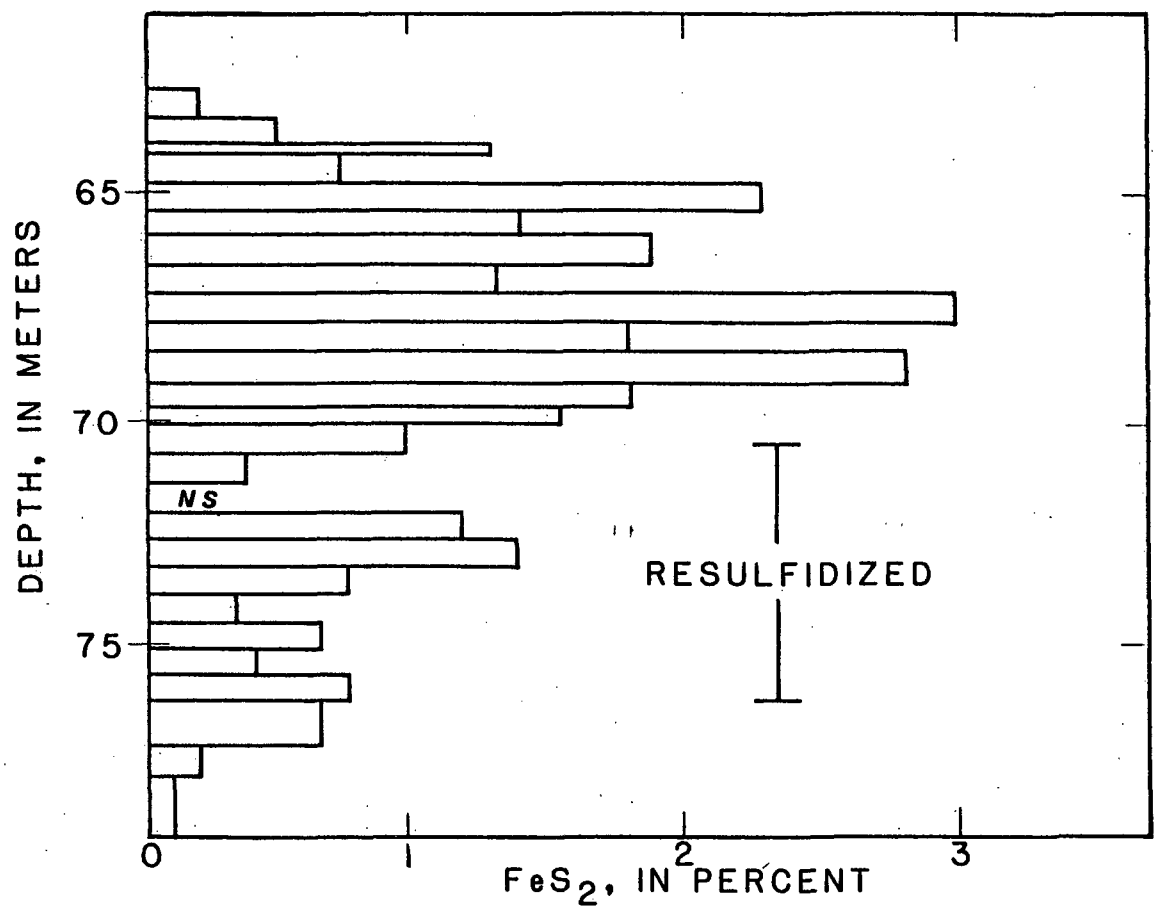

Figure 17.--Plot of weight percent iron disulfide as a function of depth in core 4. The resulfidized zone as defined by uranium (fig. 6), molybdenum (fig. 9) and selemium concretration (fig. 7) is marked for reference.

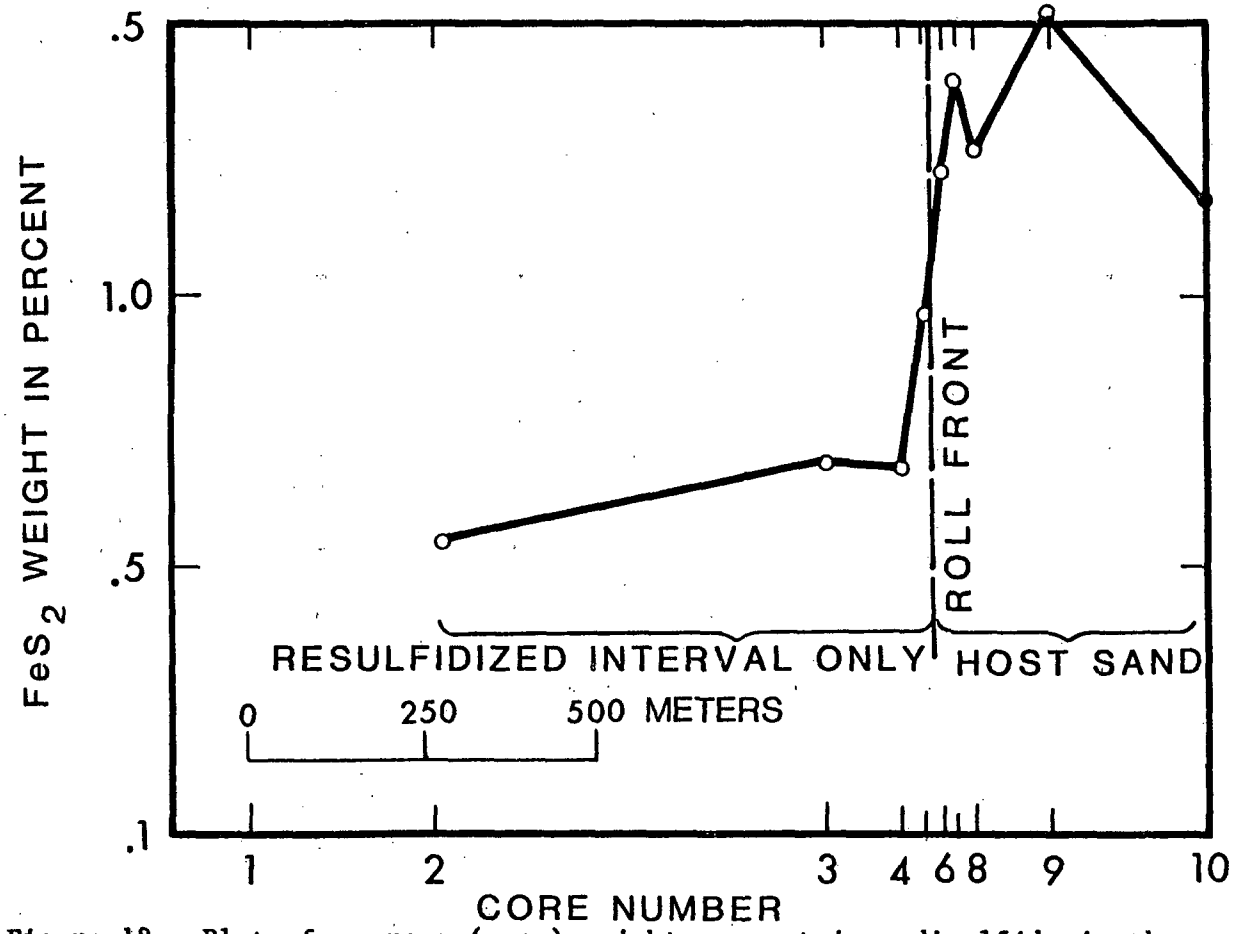

Figure 18.--Plot of average (mean) weight percent iron disulfide in the individual cores as a function of position along the core fence. The boundary between the resulfidized interval and ore roll is marked by a vertical dashed line. Updip from this boundary only data from the resulfidized interval were averaged, whereas downdip from this boundary, data from the entire host sand were averaged. The plot shows significant concentrations of iron disulfide in the resulfidized interval, although somewhat less than in other parts of the deposit.

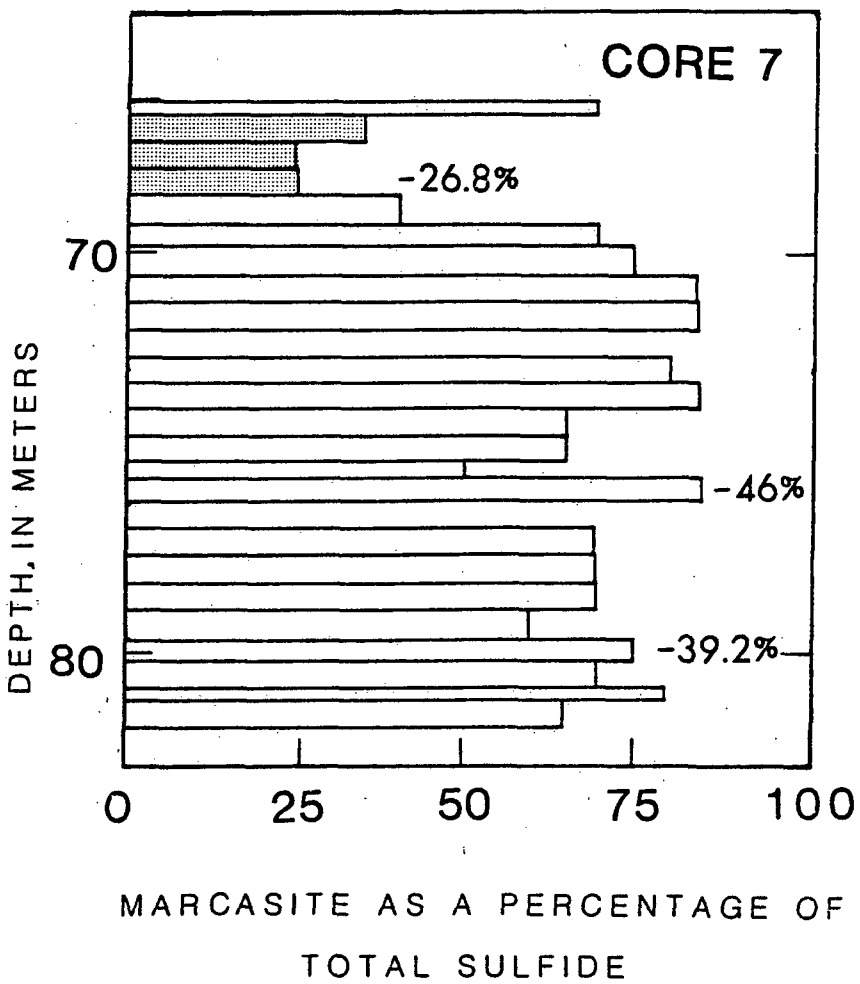

Figure 19.--Plot of the relative abundance of marcasite as a percentage of total iron disulfide mineral population (pyrite plus marcasite) against depth in core 7. Also shown are $\delta^{34}S$ values of the iron disulfides. The shaded interval denotes mudstone.

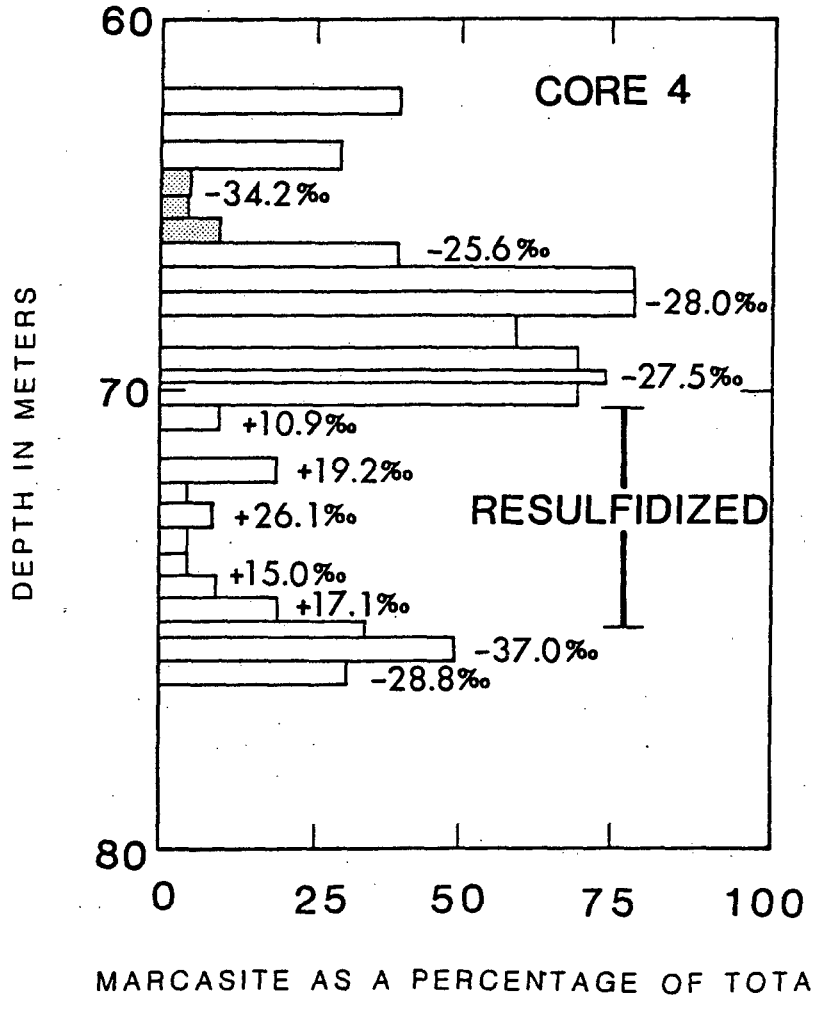

Figure 20.--Plot of the relative abundance of marcasite as a percentage of total iron disulfide mineral population (pyrite plus marcasite) against depth in core 4. The resulfidized zone is shown by the vertical bar. Note the depletion of marcasite relative to pyrite in the resulfidized interval. Also shown are $\delta^{34}S$ values of the iron disulfides illustrating the marked difference between FeS_2 minerals in resulfidized interval and those [sulfides] outside this zone. The shaded interval denotes mudstone.

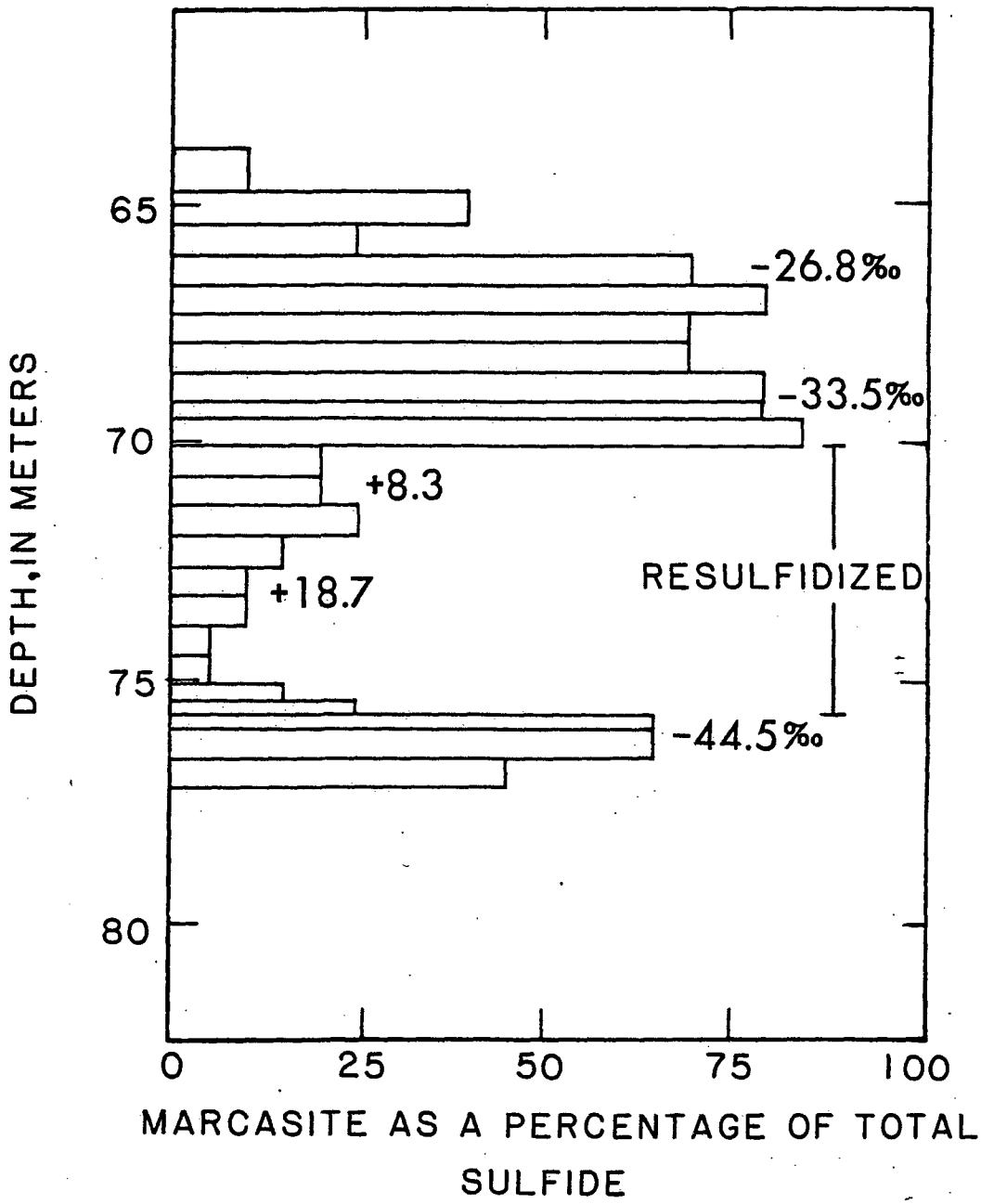

Figure 21.--Plot of the relative abundance of marcasite as a percentage of total iron-disulfide mineral population (pyrite plus marcasite) versus depth in core 5. The resulfidized zone (as defined by the vertical distribution of uranium, molybdenum and selenium) is indicated by vertical bar. Also shown are $\delta^{34}S$ values of the iron disulfide minerals.

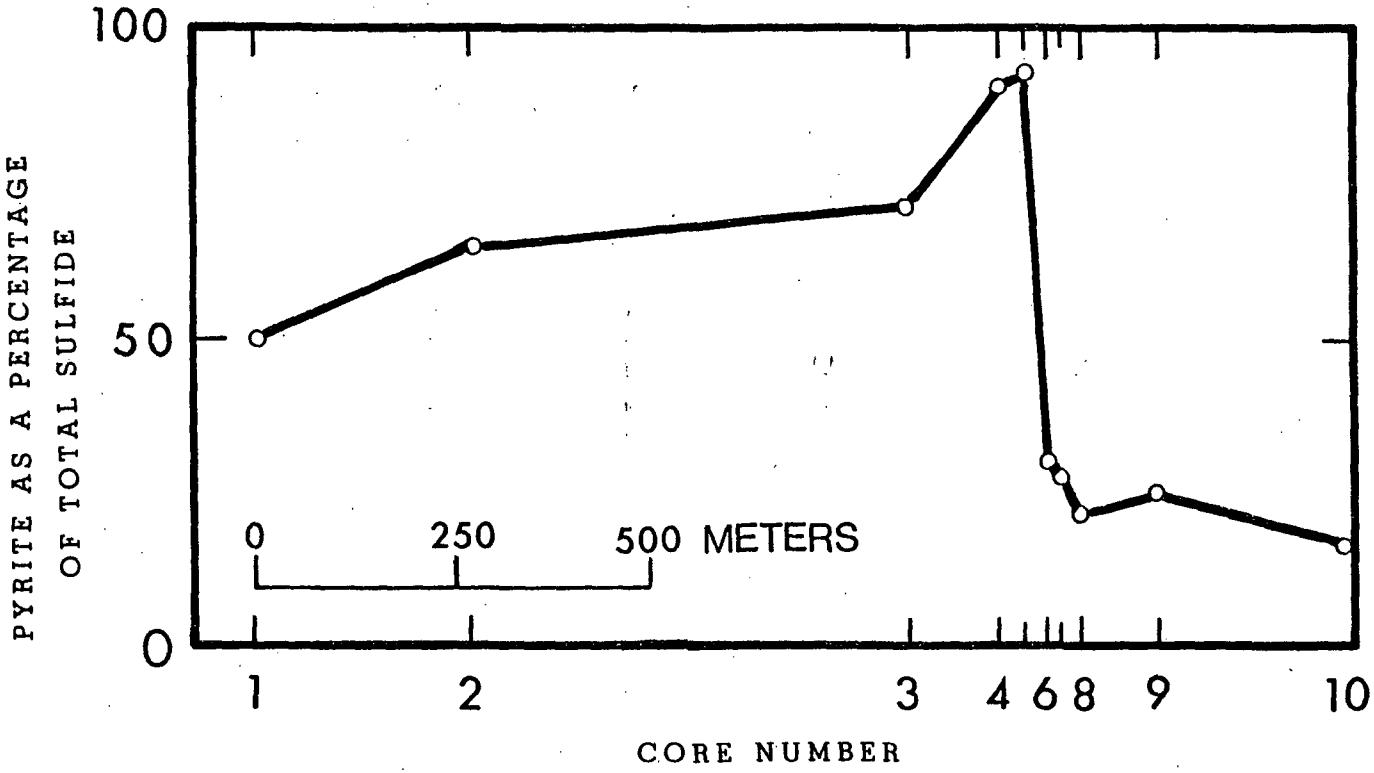

Figure 22.--Plot of the average relative abundance of pyrite as a percentage of the total iron disulfide mineral population (pyrite plus marcasite) against core position along the core fence. For cores 1 to 5, only the resulfidized portion of the host sand was considered, whereas for cores 6 to 10 data from the entire thickness of the host sand was averaged. The plot illustrates the marked discrepancy in sulfide mineralogy between resulfidized and other portions of the deposit.

and euhedral pyrite crystals and iron-titanium (Fe-Ti) oxide minerals replaced completely or partly by pyrite. Marcasite by itself or together with pyrite may also replace the Fe-Ti oxides. Also present in this portion of the host beds and extremely abundant in the upper mudstone are aggregates of small (5-20 m across) pyrite cubes. Similar clusters of pyrite cubes that occur in silt and sand beds, near and in limb ore, are cemented by a later generation of marcasite.

Within the resulfidized interval in cores 3,4, and 5, pyrite as large euhedral crystals and cement is by far the dominant sulfide occurrence. The clusters of pyrite cubes are absent. Single crystals of marcasite may be present but are rare. In the upper and lower parts of the resulfidized zone in cores 3 and 4 and throughout the zone in core 5, marcasite occurs also as thin (as much as 10 μm) rims on anhedral to euhedral grains of pyrite. As is evident from the earlier discussion of sulfide abundance (figs. 20, 21), marcasite in this form is volumetrically very minor. We have discussed previously evidence that points to the earlier presence of an oxidized tongue in what is now the resulfidized interval. It is likely then that most iron disulfide minerals in this zone represent the last sulfide generation and are equivalent in time to the latest sulfide (dominantly pyrite rims on marcasite) that is seen above and below the resulfidized zone in cores 3, 4, and 5. Unlike the thick and distinct marcasite rims above and below the resulfidized zone, the thin marcasite overgrowths in the resulfidized zone may have formed during the last episode of sulfidization. However, remnant pre-ore or ore-stage sulfides would be present in the resulfidized zone if protected from or incompletely destroyed by ore-bearing solutions.

Iron-disulfide minerals from samples in cores downdip from the roll front (core 6 through 10) display textural relations fundamentally similar to those in samples outside the resulfidized zone in cores 3, 4, and 5. Clusters of small pyrite crystals are common in mudstone and where observed in silt and sand beds are cemented by younger marcasite. Marcasite also surrounds larger pyrite crystals and Fe-Ti oxides and rock fragments that have been replaced by pyrite or by pyrite and marcasite. Euhedral and subhedral marcasite grains are the dominant sulfide minerals in rock downdip from the ore roll. Intergrowths of pyrite within marcasite grains and within marcasite overgrowths are also present but are more abundant in cores 9 and 10 than in cores 6, 7, and 8. This texture may represent contemporaneous precipitation of pyrite and marcasite. Pyrite representing the last sulfide generation occurs as overgrowths on individual marcasite grains, on marcasite overgrowth rims, and on grains of intergrown pyrite and marcasite in each of the cores downdip from the ore roll. This pyrite is probably correlative with the pyrite seen in the resulfidized interval, but it may in part represent a much later generation related to sulfide in modern ground water.

Sulfur-isotope ratios of iron disulfide minerals

Results of sulfur-isotope analyses on a selected suite of samples show a large range of 72 permil (+26 to -46) which is typical of roll-type uranium deposits (Goldhaber and others, 1978 and references cited therein). Isotopic ratios of iron disulfide minerals downdip from the nose of the roll (cores 6 to 10) are uniformly enriched in ^{32}S (fig. 19 and 23). Sulfur isotope values from the host sand in cores 6 to 10 range from -24 to -46 permil. The vertical distributions of $\delta^{34}S$ values within individual cores of this group do

not indicate any systematic trends (for example, fig. 19). Iron disulfides from the upper and lower limbs of cores that penetrate the altered tongue are also enriched in ^{32}S (figs. 20 and 21). However, samples within the resulfidized zone are strikingly enriched in ^{34}S (figs. 20 and 21), with $\delta^{34}S$ values as much as +26 permil. In figure 23, we have plotted mean values for the resulfidized interval as well as for cores 6 to 10 ahead of the roll as a function of relative core position. The contrast between the resulfidized and the remaining portions of the deposit suggests a major difference in either source of sulfur or different processes of isotopic fractionation in these two environments. One clue to the origin of this difference may be found by comparing figures 22 and 23. This comparison suggests a strong correlation between the average proportions of pyrite to total sulfide, and the averaged isotope values. This similarity is documented in figure 24. The linear relationship between these two parameters establishes the likelihood of two component mixing in which pyrite of approximately +10 permil and marcasite of -55 permil are present in varying proportions. It is important to point out, however, that averaging values from within an individual core (cores 6 to 10) or portions of a core such as the resulfidized zone (cores 1 to 5) removes considerable scatter. When the individual values are considered there is significant deviation from strict two-component mixing particularly at the marcasite end member. An additional point to note is the significant deviation of pyrite-rich samples of mudstone layers (not shown) from the trend in figure 24. The isotope data from mudstone samples are displaced towards isotopically light sulfur relative to their pyrite content (fig. 19), and pyrite in mudstone apparently formed via a different mechanism or from a different sulfur source than did pyrite in the resulfidized zone. This possibility is supported by the observation of significantly different textures in the two zones as discussed above.

Discussion

The suite of elements and their geometric relationships throughout the Lamprecht deposit are those expected for typical roll-type deposits with well developed oxidation-reduction interfaces. Yet iron-disulfide minerals are abundant in the altered tongue (resulfidized interval).

Iron disulfide minerals in the resulfidized interval differ mineralogically and isotopically from those throughout the remainder of the deposit. The resulfidized sand contains dominantly pyrite that is enriched in ^{34}S, whereas sand beyond the former altered tongue contains abundant marcasite that is enriched in ^{32}S. Textural relationships among pyrite and marcasite help to establish relative timing of iron disulfide formation. In reduced rock beyond the altered tongue, at least three distinct generations of iron-disulfide minerals are present. The oldest of these generations consists largely of pyrite with lesser amounts of marcasite. A major episode of marcasite formation (including a minor amount of pyrite) postdates the oldest iron disulfides but predates a younger generation of pyrite. Sulfidization of the altered tongue (resulfidization) resulted in pyrite that we interpret to be at least in part equivalent to the youngest pyrite generation recognized beyond the altered tongue.

In order to understand the data from the Lamprecht deposit, it is helpful to review results and conclusions from similar study on a deposit that has not been resulfidized--the Benavides deposit in the Catahoula Tuff, near Bruni,

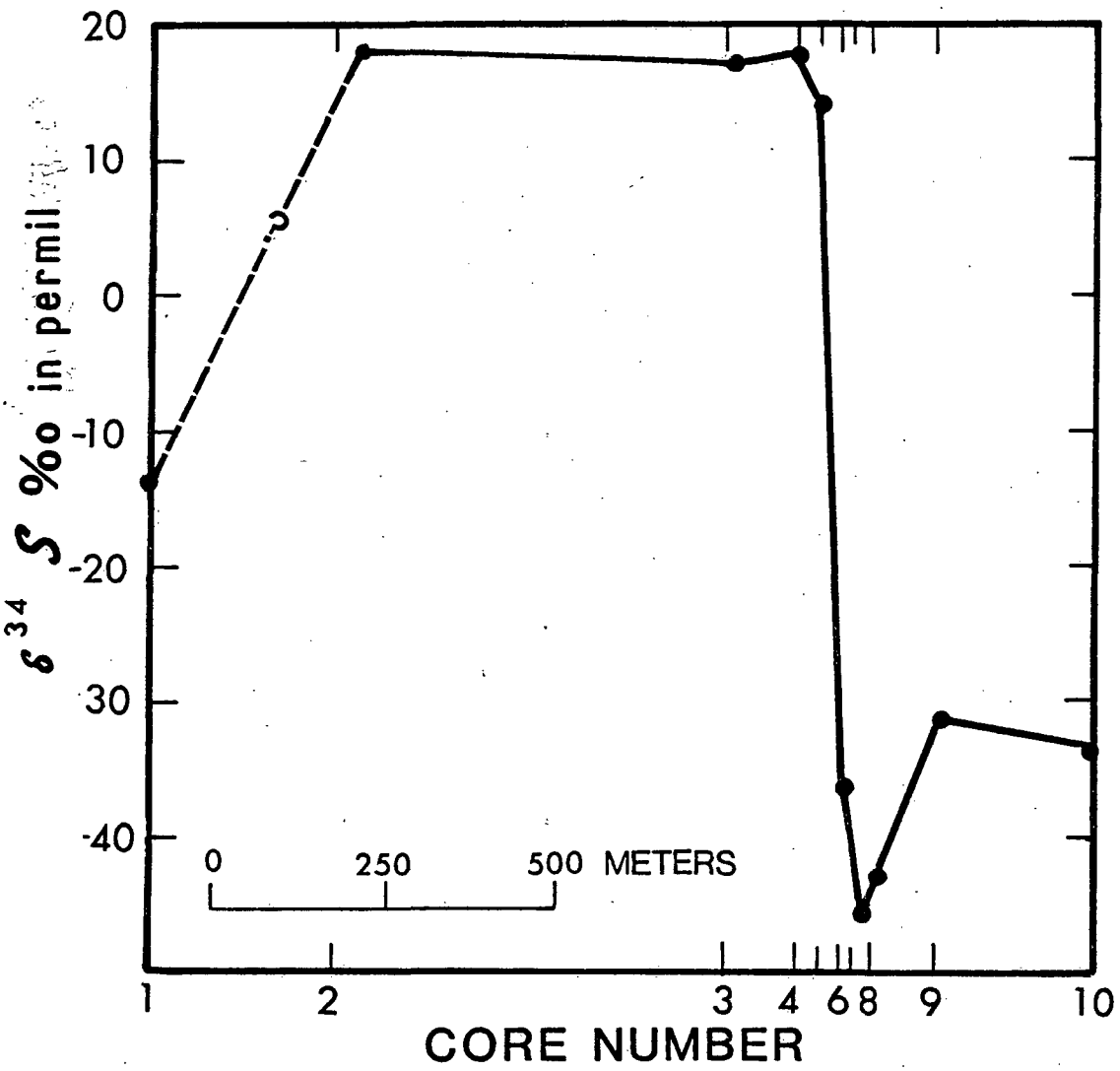

Figure 23.--Plot of averaged $\delta^{34}S$ values of iron disulfide minerals for samples distributed as in figure 22, illustrating the marked difference in isotope ratio between resulfidized and the remaining portions of the deposit. The line between data points for cores 1 and 2 is dashed because of the very limited sample interval for core 1.

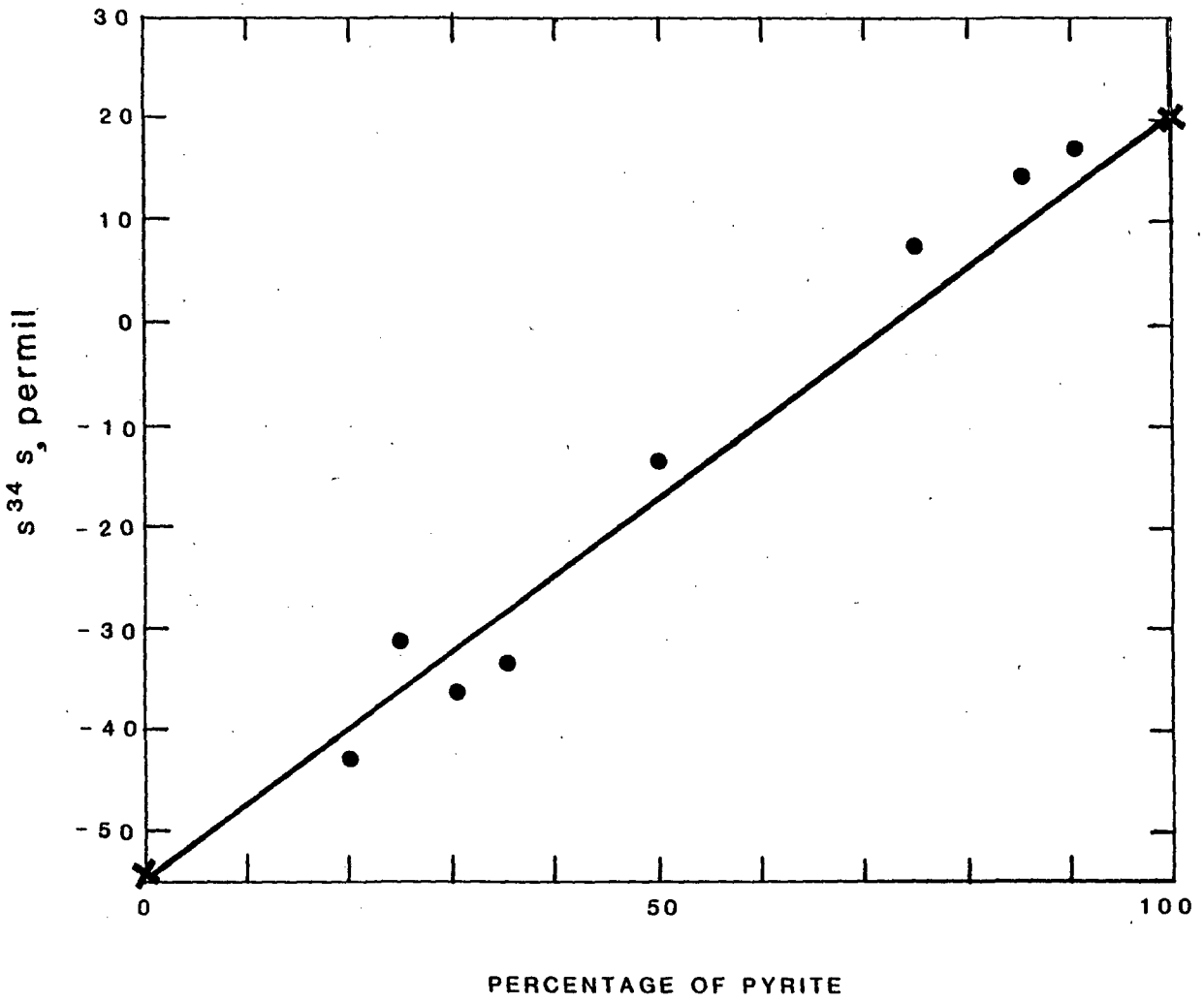

Figure 24.--Plot of mean values of relative pyrite abundance from figure 22 versus the mean sulfur isotope ratio from figure 23 illustrating the possibility of two component mixing between sulfur with an isotope value of -55 permil and a second source with a value of +20 permil.

Webb County, Texas (Reynolds and Goldhaber, 1978, Goldhaber and others, 1978). That study established the following sequence of events. An initial stage of sulfidization resulted from aqueous sulfide moving updip away from a nearby normal fault. The product of this sulfidization was dominantly pyrite. It was also established that this early fault-derived sulfur was isotopically heavy (+15 permil). The initial sulfidization was followed by a second and discrete episode in which marcasite was the dominant sulfide formed. This marcasite was observed commonly as overgrowths on earlier pyrite. Marcasite deposition coincided with uranium deposition in both time and space. The sulfur isotopic composition of the marcasite was very light ($\delta^{34}S$ of -25 to -35 permil).

There are important similarities between the Lamprecht and Benavides deposits that we believe are indicative of an overall similarity in genetic mechanism for these two ore bodies. The comparable features are: (1) An early pyrite stage; (2) virtual absence of organic carbon in the sediments; (3) possible fault control of the H_2S for sulfidization of iron-bearing phases; and (4) similar textures and distribution of marcasite.

The earliest iron disulfide to form in each deposit was dominantly pyrite. In the Benavides deposit this pyrite formed from fault derived H_2S and HS^- by sulfidization of iron-titanium oxide minerals prior to mineralization. For Lamprecht, the same time relationship of the oldest sulfide generation to the ore forming process is suggested by textures of FeS_2 minerals although we cannot prove a close relationship between the Oakville fault and this early pyrite.

The suggestion that the earliest pyrite generation in host rock of the Lamprecht deposit predated mineralization is supported also by petrographic observations of samples from other roll-type deposits in Texas and Wyoming (Reynolds and Goldhaber, 1979). These observations together with geochemical evidence (Goldhaber and others, 1978) demonstrate that marcasite formation resulted dominantly from ore-forming processes and that, in each deposit, pyrite clearly predated ore-stage marcasite.

In the absence of organic matter, it is unlikely that early biogenic pyrite formed within the ore sand in large quantities. Therefore, introduction of an extrinsic reductant such as fault-derived H_2S prior to or during mineralization must have been necessary to sulfidize the iron-titanium oxides and produce the reducing environment.

If the production of pre-ore iron disulfide minerals is related to extrinsic H_2S, this process must, in fact, predate the ore-forming process. This is because, otherwise, oxygenated uranium-bearing ground waters would sweep away sulfide-bearing, fault-derived solutions before sufficient quantities of uranium passed through the redox boundary to result in an ore deposit (Goldhaber and others, 1978). Furthermore, the inferred presence of an oxidized tongue prior to resulfidization implies the former presence of iron oxide minerals and thus suggests oxidation of pyrite, not H_2S. These relationships also point to a marked difference between the present ground-water hydrology-geochemistry and that which controlled ore deposition. The latter must have involved transport of large volumes of oxygenated uranium-, molybdenum-, and selenium-bearing water across the present trend of the ore roll, whereas the modern conditions, as documented above, do not resemble the ore-

forming regime.

The spatial relationship of the Lamprecht and several other deposits to the Oakville fault is well established (fig. 3). This is consistent with, but does not of itself prove, control of the position of the ore trend by fault-derived H_2S or FeS_2 minerals formed therefrom. A possible alternative explanation for fault control of these ore bodies might lie in modification, by the fault plane, of hydrologic flow of uranium-charged ground water during ore deposition.

An additional source of non-fault-derived pre-ore sulfide exists for the Lamprecht deposit. Early diagenetic bacterial sulfate reduction within clay-rich intervals of the Oakville Sandstone or Catahoula Formation may have resulted in aqueous sulfide. Compaction then may have expelled some of this bacterial sulfide from mudstones into the adjacent ore sand to produce early, isotopically light pyrite. Mudstone layers, as noted above, do themselves contain pyrite which is isotopically light. However, the low organic-carbon content of the mudstones as well as the reactivity of muds towards sulfide (Goldhaber and Kaplan, 1974), suggests that they were not the major sulfur source for pre-ore pyrite.

We equate the later marcasite at Lamprecht with the ore stage marcasite in the Benavides deposit. Marcasite in both ore bodies is isotopically very light. In addition, marcasite in both deposits is similar in texture, distribution and relationship to earlier pyrite. We have interpreted that the abundant ore-stage marcasite in the Benavides deposit was related to low pH attending the ore-forming episode, and that ^{32}S enrichment was also related to ore-forming processes (Goldhaber and others, 1978).

Distribution of elements as well as distribution and textures of iron disulfide minerals thoughout the Lamprecht deposit indicate that the isotopically heavy FeS_2 minerals (dominantly pyrite) in the resulfidized interval formed after uranium emplacement. Formation of the isotopically heavy iron disulfide minerals required large amounts of isotopically heavy aqueous sulfide. It is unlikely that sulfide of an appropriate isotopic composition can be derived via shallow ground-water processes of the type that presently are producing the dissolved H_2S and HS^- in the Oakville Sandstone. Rather, consideration of sulfur isotopic data on underlying oil and gas as well as local structural relationships point to deep-seated fault-derived H_2S as a likely source of sulfur for FeS_2 minerals in the resulfidized zone. Commercial quantities of natural gas associated with sulfide are found in the Edwards Limestone deep reef trend which underlies the Lamprecht deposit (fig. 1). Carbonate reservoir rocks are associated commonly with sour gas because there is little available iron to fix H_2S as FeS_2 (Dobbin, 1935). Sulfide analyses of gas from the Edwards yield values of approximately 1 percent H_2S. The $\delta^{34}S$ of H_2S from the Edwards is in the correct range for producing the observed $\delta^{34}S$ of the iron disulfide minerals in the resulfidized interval. Analyses on oil-field brines derived from the Edwards at the Jourdanton, Texas gas field (Humble Oil Company, Schorsih lease) yielded 210 ppm total dissolved sulfide with a $\delta^{34}S$ value of +14.1 permil and $\delta^{34}S$ of associated sulfate of +25.8 permil (F. J. Pearson, written commun., 1978). Elemental sulfur produced during the desulfurization (by oxidation) of sour Edwards gas (by a process which is unlikely to produce isotopic fractionation) has a $\delta^{34}S$ value of +12.2 to 12.3 permil (Austin, 1971). Other gas and

petroleum fields likewise contain isotopically heavy H_2S (fig. 25). Another major gas-producing unit in Live Oak County, the Wilcox Formation, does not contain H_2S (D. Oehler, Continental Oil Company, oral commun., 1978). Therefore, we postulate that the Oakville fault at sometime subsequent to the formation of the deposit acted as a conduit for sulfide-bearing brines from the Edwards into the Oakville Sandstone. The Oakville fault is presumably a growth fault along which movement has occurred intermittently during geologic time (Jones and Wallace, 1974). Brines from the Edwards may have been driven upward along the fault by overpressure (Jones and Wallace, 1974).

Summary and Suggestions for Exploration

Based upon evidence developed during this study, we postulate that the Lamprecht deposit formed in at least two stages:

(1) A pre-ore process of sulfidization which produced pyrite as the dominant but not exclusive iron disulfide phase. We are not able conclusively to establish the source of sulfur for this process. Fault-derived H_2S from underlying oil and gas fields, early diagenetic sulfide produced bacterially in superjacent or subjacent mudstones, and near-surface ground-water sulfate reduction such as is presently occurring in the vicinity of the mine site or some combination of these are all possibilities.

(2) An ore-stage process which led to the development of a uranium roll with emplacement of the characteristic suite of minor and accessory elements. The dominant iron disulfide mineral formed during mineralization was marcasite that occurs in part as overgrowths on pre-ore pyrite. The marcasite is isotopically light. Sulfur, from pre-ore iron disulfides that were oxidized by oxygenated, uranium-bearing solutions, was mobilized and redistributed into the present ore and reduced barren zones, where it reacted with available iron to form the ore-stage marcasite.

A post-ore process of resulfidization resulted in sulfidization of the altered (oxidized) tongue. This sulfidization produced isotopically heavy pyrite. The sulfur for this process was derived from an oil and (or) gas reservoir perhaps in the Edwards Limestone underlying the uranium deposit.

Present ground-water processes in the host rock differ greatly from those that formed the deposit. Aqueous sulfide appears to be related to the near surface bacterial or inorganic processes. Iron disulfide minerals resulting from these processes have not been unequivocally identified in the host sand of the deposit.

Formation of the Lamprecht deposit has resulted in marked geochemical and mineralogical difference perpendicular to the strike of the ore-roll. In particular, iron disulfide mineralogy (fig. 22) and sulfur isotopes (fig. 23) show marked differences between samples located updip and those downdip from ore. Such differences can clearly be applied to uranium exploration in terranes containing resulfidized rock.

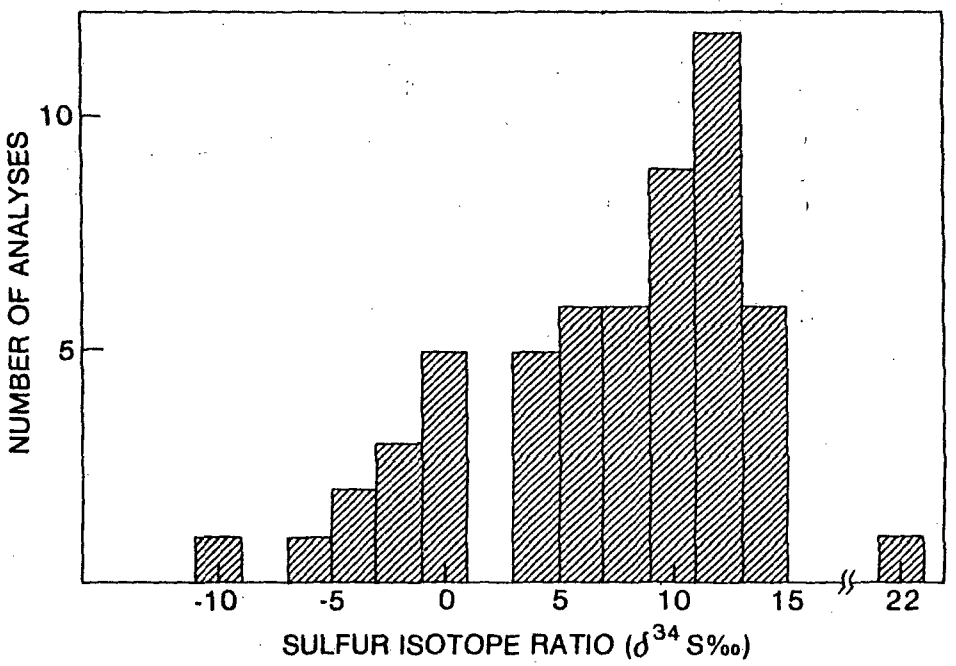

Figure 25.--Histogram showing the distribution of sulfur isotopic ratios in gaseous and aqueous sulfides associated with oil; Wind River Basin and Big Horn Basin, Wyoming and the Volga-Urals region USSR. From Goldhaber and others (1978).

References

Adler, H. H., 1974, Concepts of uranium-ore formation in reducing environments in sandstones and other sediments, in Symposium on formation of uranium ore deposits: Athens, International Atomic Energy Agency, p. 141-168.

Adler, H. H., and Sharp, B. J., 1967, Uranium ore rolls-occurrence, genesis and physical and chemical characteristics: Utah Geological Society Guidebook No. 21, p. 53-77

Austin S. R., 1971, Final tabulation of sulfur-isotope analyses: U.S. Atomic Energy Commission., AEC-RPD-13, 76 p.

Bebout, D. G., 1977, Sligo and Houston depositional patterns, subsurface of south Texas, in Bebout, D. G., and Loucks, R. G., editors, Cretaceous carbonates of Texas and Mexico: Texas Bureau of Economic Geology Report of Investigation 89, p.79-96.

Dickinson, K. A., 1976, Uranium potential of the Texas Coastal plain: U.S. Geological Survey Open-File Report 76-879, 7 p.

Dickinson, K. A., and Duval, J. S., 1977, South Texas uranium--geologic controls, exploration techniques and potentials, in M. D. Campbell, editor, Geology of alternate energy resources: Houston Geological Survey, p. 45-66.

Dobbin, C. E., 1935, Geology of natural gases rich in helium nitrogen, carbon dioxide and hydrogen sulfide, in Ley, H. A., editor, Geology of Natural Gas: American Association of Petroleum Geologists Symposium, p. 1053-1072.

Eargle, D. H., and Weeks, A. M. D., 1961, Possible relation between hydrogen sulfide-bearing hydrocarbons in fault line oil fields and uranium deposits in the southeast Texas coastal plain: U.S. Geological Survey Professional Paper 424D, p. 7-9.

Galloway, W. E., 1977, Catahoula Formation of the Texas Coastal Plain: depositional systems, composition, structural development, ground water flow history and uranium distribution: Texas Bureau of Economic Geology, Report of Investigation 87, 59 p.

Goldhaber, M. B., 1974, Equilibrium and dynamic aspects of the marine geochemistry of sulfur: University of California at Los Angeles, unpub. Ph.D. thesis, 399 p.

Goldhaber, M. B., and Kaplan, I. R., 1974, The sulfur cycle, in The Sea, Volume V, Marine Chemistry, Goldberg, E., editor: New York, John Wiley and Sons, Inc., p. 569-655.

Goldhaber, M. B., Reynolds, R. L., and Rye, R. O., 1978, Origin of a south Texas roll-type uranium deposit, Part 2--Sulfide petrology and sulfur isotopic studies: Economic Geology, v. 73 p. 1690-1705.

Granger, H. C., and Warren, C. G., 1969, Unstable sulfur compounds and the origin of roll-type uranium deposits: Economic Geology, v. 64, p. 160-171.

Harshman, E. N., 1974, Distribution of elements in some roll-type uranium deposits, in Formation of uranium ore deposits: Vienna, International Atomic Energy Agency, Proceedings, 1974, p. 169-183.

Jones, P. H., and Wallace, R. H. Jr., 1974, Hydrogeologic aspects of structural deformation in the northern Gulf of Mexico basin: U.S. Geological Survey, Journal of Research, v. 2, p. 511-517.

Klohn, M. L., and Pickens, W. R., 1970, Geology of the Felder uranium deposit, Live Oak County, Texas: Mining Engineers Society preprint no. 70-1-38, 19 p.

Orr, W. L., 1974, Changes in sulfur content and isotopic ratios of sulfur during petroleum maturation--study of Big Horn Basin Paleozoic oils: Americal Association of Petroleum Geologists Bulletin, v. 50, p. 2295-2318.

Rackley, R. I., 1972, Environment of Wyoming Tertiary uranium deposits: American Association of Petroleum Geologists Bulletin, v. 56, p. 755-774.

Reynolds, R. L., and Goldhaber, M. B., 1978, Origin of a south Texas roll-type uranium deposit; Part I--Alteration of iron-titanium oxide minerals: Economic Geology, v. 73, p. 1677-1689.

Reynolds, R. L., and Goldhaber, M. B., 1979, Marcasite in roll-type uranium deposits [abs.]: American Association of Petroleum Geologists Annual Meeting Program, p. 150-151.

Rightmire C. T., Pearson, F. J. Jr., Back W., Rye, R. O., and Harshaw, B. B., 1974, Distribution of sulfur isotopes of sulfates in groundwaters from the principal artesian aquifer of Florida and the Edwards aquifer of Texas, United States of America: International Atomic Energy Agency Symposium, 182/39, p. 191-207.

Rinehart, I., 1962, South Texas Edwards trend exploration, Rinehart Oil News Company, Dallas, Texas, p. 3.